diameter, left atrial diameter, and indexes of systolic function), as well as E/A (an index of the diastolic function), which was the focus of this study. These parameters were analyzed in relation to age. The aging-related changes in E/A were also analyzed for 394 normotensive individuals with intact hearts who were found to have no organic heart disease when examined by echocardiography (the control group, composed of 164 men and 230 women, with a mean age of 57.5 ± 15.0 years). The data from the HT group were compared with those from the control group.

In the HT group, left ventricular (LV) mass was measured by M-mode echocardiography of the left ventricle under 2-D guidance. This mass was divided by the body surface area to yield the LV mass index. The sum total of the ventricular septum thickness and the left ventricular posterior wall thickness was divided by the left ventricular end-diastolic diameter to yield relative wall thickness. When the pattern of cardiac hypertrophy was analyzed using these two parameters (LV mass index and relative wall thickness), with the cut-off level set at 110 g/m^2 and 0.44, respectively,[5] 44.5% of the patients were rated as having concentric hypertrophy, 33.9% as having eccentric hypertrophy, 5.0% as having concentric remodeling, and 16.5% as having normal morphology.

The devices used for ultrasonographic data collection in the present study were Sonos-5500 (Philips Medical Systems, Andover, Mass), SSD-2200 (Aloka, Tokyo, Japan), SSD-5500 (Aloka, Tokyo, Japan), SSD-6500 (Aloka, Tokyo, Japan), and System FiVe (GE-Vingmed, Horten, Norway), which were available for clinical use at our facility at the time of the study. These devices were used in combination with 2.5–3.75-MHz transducers.

Patients with myocardial infarction (acute or old), hypertrophic cardiomyopathy, dilated cardiomyopathy, restrictive cardiomyopathy, pericardial disease, significant valvular heart disease, atrial fibrillation, or implanted pacemakers were excluded from the study. Patients in cardiac failure at the time of echocardiography were also excluded from the study.

In statistical analysis of data, analysis of variance (ANOVA) was used for inter-group and age-wise comparisons of continuous variables, and the Scheffe method was used for post-hoc testing. Analysis was conducted by using the StatView for Windows software (version 5.0, SAS Institute Inc.). $P < 0.05$ was regarded as statistically significant. Regression analysis of age and E/A was conducted. This study was approved by the Institutional Review Board of Yamaguchi University Hospital before it began.

Results

Table 1 shows the age and other background variables of the subjects. The mean age was approximately 9 years older in the HT group than in the control group. This large difference in age made it difficult for us to make simple comparisons of data between the HT and the control groups. For this reason, we attempted comparisons between the HT group and the control group by subdividing each group according to age.

Table 1. Characteristics of the subjects

	HT group (n = 553)	Control group (n = 394)
Age (years)	66.0 ± 11.2	57.5 ± 15.0
Sex (male/female)	290/263	164/230
Systolic BP (mmHg)	148 ± 19	122 ± 15
Diastolic BP (mmHg)	85 ± 12	74 ± 10
LVDd (mm)	47.2 ± 4.1	45.8 ± 3.5
LVDs (mm)	27.9 ± 4.1	27.7 ± 3.7
%FS (%)	41.1 ± 6.5	39.6 ± 5.7
LVEF (%)	71.0 ± 6.8	69.6 ± 6.4
Aortic root diameter (mm)	31.8 ± 4.6	29.5 ± 4.1
LA dimension (mm)	37.6 ± 6.1	33.7 ± 5.3
E (m/s)	0.61 ± 0.16	0.64 ± 0.16
A (m/s)	0.78 ± 0.19	0.63 ± 0.19
E/A	0.82 ± 0.34	1.11 ± 0.53

BP, blood pressure; LVDd, left ventricular internal diameter at end-diastole; LVDs, left ventricular internal diameter at end-systole; %FS, fractional shortening; LVEF, left ventricular ejection fraction; LA, left atrium; E, early diastolic flow velocity of transmitral flow; A, late diastolic flow velocity of transmitral flow. Values are means ± SD

In subjects older than 30 years, the mean left ventricular end-diastolic diameter tended to be slightly greater in the HT group than in the control group. However, there was no statistically significant difference in this parameter between the HT patients and the healthy controls in any age group. There were no significant differences between the control group and the HT group or between any two age groups with respect to left ventricular end-systolic diameter (Fig. 1a,b).

The mean left ventricular ejection fraction, an index of systolic function, was greater than 60% in each age group in both the HT and the control groups, indicating that systolic function was preserved in all groups. When subjects were analyzed by age, there was no significant difference in this parameter between the HT group and the control group (Fig. 1c).

The mean left atrial diameter was slightly greater in the HT patients than in the healthy controls in all age groups. However, the difference was significant only in the 50–59 years age group (Fig. 1d).

The E/A ratio of transmitral flow, an index of diastolic function, tended to decrease gradually with age in both the control group and the HT group. In the control group, the mean ratio was <1 at age 60–69 years. But in the HT group, the ratio had already decreased significantly by age 30–39, it was still lower in the 40–49 years age group, and it was <1 at age 50–59, which was earlier than in the control group (Fig. 2).

When a regression line was drawn for both the control group and the HT group for the relationship between E/A ratio and age, the E/A ratio became <1 at age 63.2 years on the regression line ($y = -0.021x + 2.328$; $r = 0.67$) in the control group, and the ratio became <1 at age 50.3 years ($y = -0.012x + 1.604$; $r = 0.43$) in the HT group (Fig. 3). Thus, in terms of mean E/A ratio, the relationship between E and A was reversed approximately 13 years earlier in the HT group than in the control group.

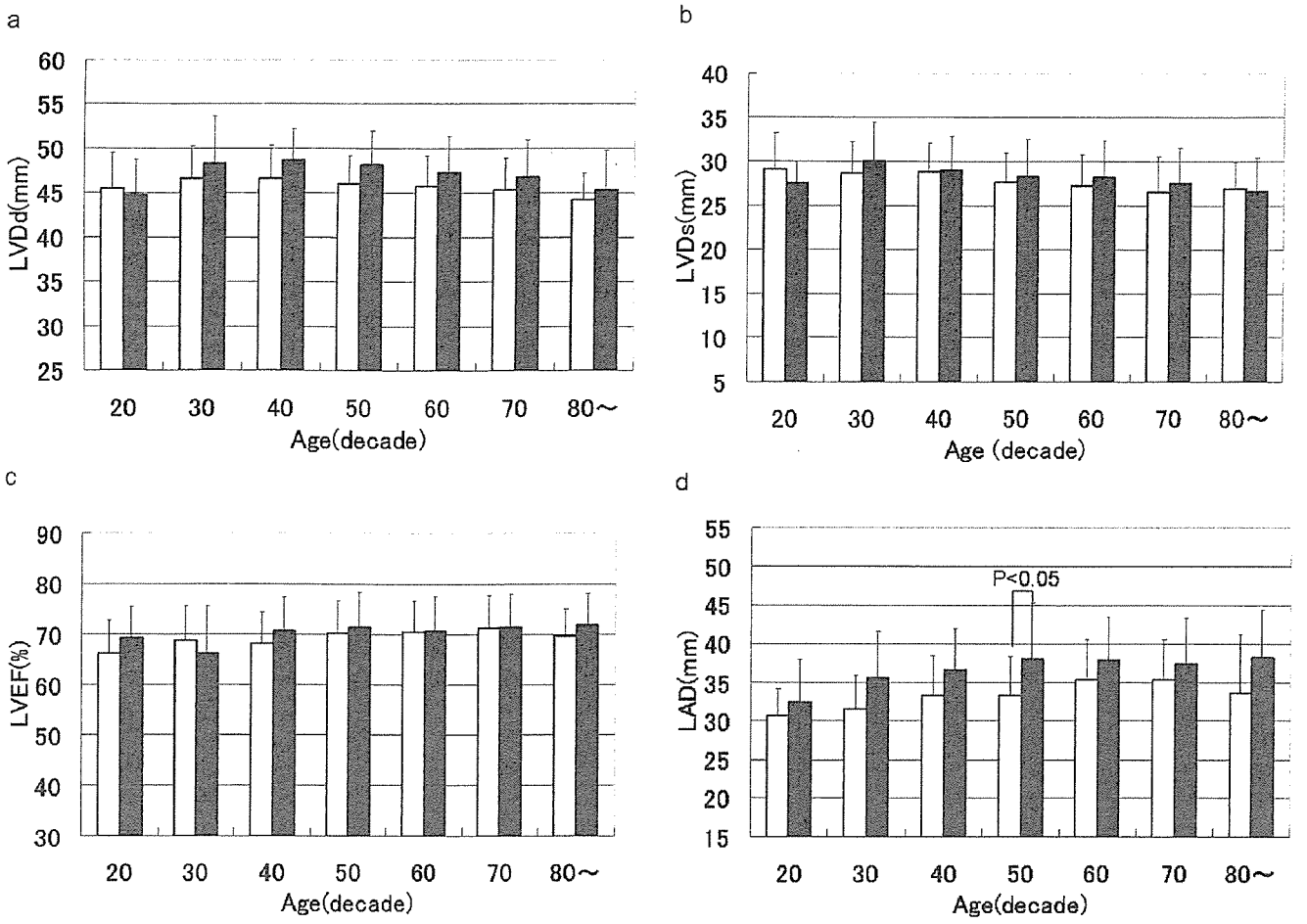

Fig. 1a–d. Relationship between echocardiographic measurements and aging in subjects with or without hypertension. **a** Left ventricular internal diameter at end-diastole (LVDd); **b** left ventricular internal diameter at end-systole (LVDs); **c** left ventricular ejection fraction (LVEF); **d** left atrial diameter (LAD). *Open* and *solid bars* indicate normal subjects and patients with hypertension, respectively. Values are mean ± SD

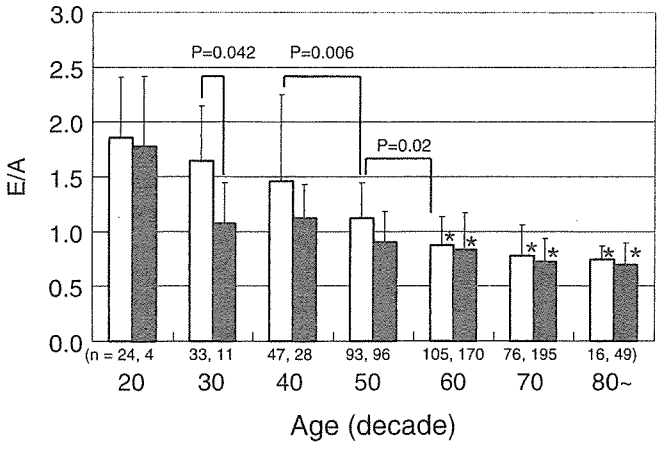

Fig. 2. Changes in E/A ratio of transmitral flow with aging in subjects with or without hypertension. The *number* just below each *bar* indicates the number of subjects in each category. *Asterisks*, $P < 0.025$ vs. bar at age 20 of each category

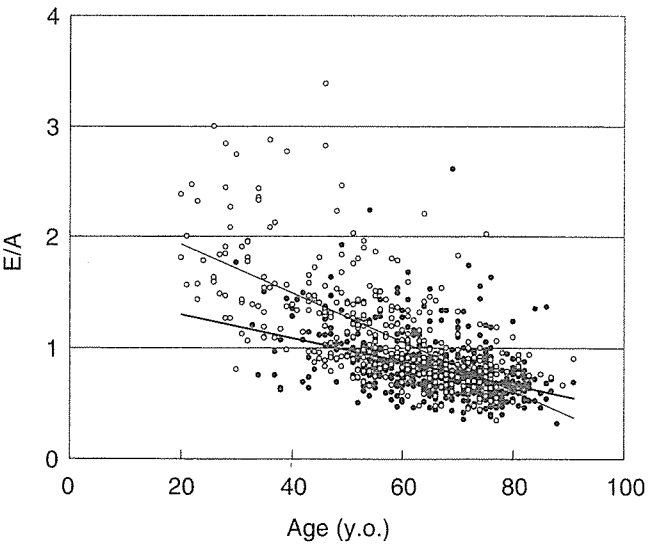

Fig. 3. Regression analysis between E/A and age in normal subjects (*open circles* and *thin line*: $y = -0.021x + 2.328$, $r = 0.67$) and patients with hypertension (*closed circles* and *thick line*: $y = -0.012x + 1.604$, $r = 0.43$)

Discussion

The E/A ratio of transmitral flow (TMF) is a simple index of diastolic function that is often used in clinical practice.[1–4] TMF is determined primarily by the left atrium-left ventricle pressure gradient in diastole, and it is known that the changes in its pattern reflect left ventricular diastolic function. However, TMF can be affected by loading conditions. For example, it is known that pseudonormalization patterns can be seen in TMF patterns, thus limiting the usefulness of the TMF pattern as a means of evaluation of diastolic function. To overcome this problem, diastolic function is sometimes evaluated on the basis of TMF pattern in combination with pulmonary venous flow pattern, propagation velocity of the left ventricular inflow, tissue Doppler data, and other factors, instead of on the basis of TMF pattern alone. In addition to this problem, it is also known that TMF can be affected by aging.[6–8] The results of the present study also emphasize the necessity of taking age into account when interpreting E/A values.

Spirito and Maron[6] conducted a study using volunteers from 20 to 74 years old who were free of evident heart disease and without a history of hypertension, and found that the E/A of TMF decreased with age, with the E/A dipping below 1 in the middle of the sixth decade as assessed on the regression line. In this age group, prolonged isovolumetric relaxation time and slower reduction of E wave velocity at early diastole were also observed, probably reflecting delayed left ventricular filling. Although the present study did not include measurement of the isovolumetric relaxation time, the age-related course of E/A in Spirito and Maron's study suggests that the age-related changes observed in our healthy controls, who were free of organic heart disease, also reflect the delayed left ventricular filling due to aging, similar to the finding reported by Spirito and Maron.[6]

TMF is affected not by any single factor but by a combination of multiple factors, such as the characteristics of the myocardium, myocardial mass, left ventricular volume, systolic function, heart rate, and loading conditions. For example, Kitzman et al., who studied healthy individuals without evident disease history or a history of hypertension,[7] reported that, other than the peak filling rate, only age served as a significant factor affecting E or E/A of TMF. Manca et al. reported that in both healthy control subjects and hypertensive patients, left ventricular filling, as assessed on the basis of E/A, was primarily affected by age.[8]

In both young and elderly patients with hypertension, the left ventricular filling time is prolonged, and this change is seen also in the stage of disease prior to the onset of left ventricular hypertrophy.[9] Because prolonged left ventricular filling time is seen in elderly individuals with normal left ventricular myocardial mass as well as in younger individuals with increased left ventricular myocardial mass, some investigators have concluded that aging is more closely involved in the prolongation of left ventricular filling time than is left ventricular mass.[8] In any event, it is now evident that TMF can be affected to a large extent by age. Therefore, when determining a criterion range of E/A, we need to take age into account.

Hypertension can be a factor responsible for diastolic heart failure. According to a past study of hypertensive patients with a mean age of approximately 50 years,[10] a delayed relaxation pattern (E < A) can be seen even in individuals with a normal left ventricular ejection fraction, as seen in the present study. It seems likely, therefore, that in hypertensive hearts, diastolic function is disturbed earlier than systolic function. In view of the report that E/A affects the prognosis of essential hypertension,[11] we can say that E/A is a clinically significant indicator, even though it can be measured relatively easily. In recent years, indicators used in tissue Doppler studies (e.g. mitral annulus velocity along the long axis of the left ventricle) have begun to be used for evaluation of left ventricular diastolic function. A study of mitral annulus velocity E′ and E/E′ in healthy volunteers[12] revealed that these parameters were also clearly affected by age, and that E′ decreased with age, whereas E/E′ tended to increase with age.

When we analyzed parameters other than E/A of TMF in the present study, the left atrial diameter was found to be greater in HT patients than in healthy controls in all age groups. The greater left atrial diameter seems to reflect reduced left ventricular compliance, but in this respect, it has been previously reported that the left atrial diameter is associated with the prognosis of patients with dilated cardiomyopathy or hypertrophic cardiomyopathy.[13,14] In hypertensive patients, particularly hypertensive men, it has been reported that the left atrial diameter correlates with the degree of obesity and the left ventricular myocardial mass,[15] and serves as a predictor of the risk of stroke or atrial fibrillation.[16,17] However, in the present study, in which data at a single point in time were analyzed, it is not possible to discuss the relationship of these parameters to prognosis.

The data used for the present study were derived from an echocardiographic database. It was not possible in the present study to compare the data on indexes of diastolic function with other data that can be yielded only by invasive tests (e.g. intracardiac pressure). However, no previous reports have analyzed E/A data from such a large number of Japanese people as was done in the present study. We therefore report the results of this study as one piece of evidence.

Diabetes mellitus often complicates hypertension, and is a factor possibly affecting left ventricular diastolic function. In the present study, we did not exclude diabetic patients, but conducted no analysis in relation to diabetes mellitus. This is one limitation of the present study.

Conclusion

The present study revealed that an age-related change in E/A takes place more than 10 years earlier in hypertensive patients than in healthy individuals without heart disease. We plan to carry out more detailed analyses of diastolic function indicators in hypertensive patients in the future.

Acknowledgment This study was partly supported by a Grant-in-Aid for Scientific Research (17500330) from the Ministry of Education, Culture, Sports, Science and Technology of Japan.

References

1. Kitabatake A, Inoue M, Asao M, et al. Transmitral blood flow reflecting diastolic behavior of the left ventricle in health and disease. A study by pulsed Doppler technique. Jpn Circ J 1982;46: 92–102.
2. Nishimura RA, Tajik AJ. Evaluation of diastolic filling of left ventricle in health and disease: Doppler echocardiography is the clinician's Rosetta Stone. J Am Coll Cardiol 1997;30:8–18.
3. Cohen GI, Pietrolungo JF, Thomas JD, et al. A practical guide to assessment of ventricular diastolic function using Doppler echocardiography. J Am Coll Cardiol 1996;27:1753–60.
4. Appleton CP, Hatle LK, Popp RL. Relation of transmitral flow velocity patterns to left ventricular diastolic function: new insights from a combined hemodynamic and Doppler echocardiographic study. J Am Coll Cardiol 1988;12:426–40.
5. Ganau A, Devereux RB, Roman MJ, et al. Patterns of left ventricular hypertrophy and geometric remodeling in essential hypertension. J Am Coll Cardiol 1992;19:1550–8.
6. Spirito P, Maron BJ. Influence of aging on Doppler echocardiographic indicies of left ventricular diastolic function. Br Heart J 1988;59:672–9.
7. Kitzman DW, Sheikh KH, Beere PA, et al. Age-related alterations of Doppler left ventricular filling indexes in normal subjects are independent of left ventricular mass, heart rate, contractility and loading conditions. J Am Coll Cardiol 1991;18:1243–50.
8. Manca C, Aschieri D, Piazza A, et al. Effect of aging on left ventricular filling in untreated hypertensive patients. Intern J Cardiol 1995;48:1221–9.
9. Grodzicki T, Michalewicz L, Messerli FH. Aging and essential hypertension. Effect of left ventricular hypertrophy on cardiac function. Am J Hypertension 1998;11:425–8.
10. de Simone G, Greco R, Muressu GF, et al. Relation of left ventricular diastolic properties to systolic function in arterial hypertension. Circulation 2000;101:152–7.
11. Schillaci G, Pasqualini L, Verdecchia P, et al. Prognostic significance of left ventricular diastolic dysfunction in essential hypertension. J Am Coll Cardiol 2002;39:2005–11.
12. Tighe DA, Vinch CS, Hill JC, et al. Influence of age on assessment of diastolic function by Doppler tissue imaging. Am J Cardiol 2003;91:254–7.
13. Rossi A, Cicoira M, Zanolla L, et al. Determinants and prognostic value of left atrial volume in patients with dilated cardiomyopathy. J Am Coll Cardiol 2002;40:1425–30.
14. Maron BJ. Hypertrophic cardiomyopathy. A systematic review. JAMA 2002;287:1308–20.
15. Gottdiener JS, Reda DJ, Williams DW, et al. Left atrial size in hypertensive men: influence of obesity, race, and age. J Am Coll Cardiol 1997;29:651–8.
16. Benjamin EJ, D'Agostino RB, Belanger AJ, et al. Left atrial size and the risk of stroke and death. Circulation 1995;92:835–41.
17. Henry W, Morganroth J, Pearlman A, et al. Relation between echocardiographically determined left atrial size and atrial fibrillation. Circulation 1976;53:273–9.

Original Article

High Ambient Pressure Produces Hypertrophy and Up-Regulates Cardiac Sarcoplasmic Reticulum Ca^{2+} Regulatory Proteins in Cultured Rat Cardiomyocytes

Takashi SATO[1], Tomoko OHKUSA[1], Shinsuke SUZUKI[1], Tomoko NAO[1], Masafumi YANO[1], and Masunori MATSUZAKI[1]

Previously, we demonstrated *in vivo* that the nature of the alterations in sarcoplasmic reticulum (SR) function and SR Ca^{2+} regulatory proteins depends both on the type of mechanical overload imposed and on the duration of the heart disorder. The purpose of the present study was to determine *in vitro* whether an extrinsic mechanical overload (in the form of high ambient pressure) would cause an up-regulation of ryanodine receptor (RyR) and Ca^{2+}-ATPase, as we previously reported mildly pressure-overloaded, hypertrophied rat hearts. Primary cultures of neonatal rat cardiomyocytes were prepared and high ambient pressure was produced using an incubator and pressure-overloading apparatus. Cells were exposed to one of two conditions for 72 h: atmospheric pressure conditions (APC) or high pressure conditions (HPC; HPC=APC+200 mmHg). The expression levels of RyR and Ca^{2+}-ATPase were quantified and functional characteristics were monitored. The cell area was significantly greater under HPC. After 6 h exposure, the physiological properties of cardiomyocytes were impaired, but they returned to the baseline level within 24 h. After 24 h exposure, the expression level of RyR was significantly higher under HPC, and for Ca^{2+}-ATPase, the expression level was significantly higher under HPC after 6 h exposure. HPC caused hypertrophy and up-regulated the expression of Ca^{2+} regulatory proteins and their genes. We suggest that this *in vitro* pressure-overloading model may prove useful, as is a stretch-overloading model, for investigation of the intracellular Ca^{2+} regulatory pathways responsible for the development of cardiac hypertrophy. (*Hypertens Res* 2006; 29: 1013–1020)

Key Words: **cardiomyocyte, pressure-overload, hypertrophy, ryanodine receptor, Ca^{2+}-ATPase**

Introduction

The cardiac sarcoplasmic reticulum (SR) plays an important role in excitation-contraction (E-C) coupling and, consequently, abnormalities of its Ca^{2+} release and uptake functions may result in systolic and diastolic dysfunctions, as in cardiac hypertrophy and heart failure. The contraction of cardiomyocytes is triggered by Ca^{2+} release from the SR, *via* a Ca^{2+} release channel that is also referred to as the ryanodine receptor (RyR). Their subsequent relaxation is initiated by an ATP-dependent transport of Ca^{2+} (*via* Ca^{2+}-ATPase) back into SR. Alterations in Ca^{2+} transport by the SR have been reported to be a cause of the altered cardiac function seen in cardiac hypertrophy and heart failure (*1*, *2*). A number of groups have identified a decrease in the level of RyR and an SR Ca^{2+}-

From the [1]Division of Cardiology, Department of Medicine and Clinical Science, Yamaguchi University Graduate School of Medicine, Ube, Japan.
This work was supported in part by a Grant-in-Aid for Scientific Research (No. C17590738) from the Ministry of Education, Cuture, Sports, Science and Technology, Japan.
Address for Reprints: Tomoko Ohkusa, M.D., Ph.D., Division of Cardiology, Department of Medicine and Clinical Science, Yamaguchi University Graduate School of Medicine, 1–1–1, Minami-kogushi, Ube 755–8505, Japan. E-mail: ohkusa@yamaguchi-u.ac.jp
Received May 1, 2006; Accepted in revised form August 9, 2006.

Table 1. Effects of Pressure-Overload on Cell Area (μm^2)

	APC	HPC
0 h	565±78	
6 h	564±93	835±154*,#
12 h	678±134#	931±162*,#
24 h	726±157#	993±245*,#
48 h	602±137	830±211*,#
72 h	633±144#	769±188*,#

APC, atmospheric pressure conditions; HPC, high pressure conditions. *$p<0.01$ *vs.* APC, #$p<0.05$ *vs.* 0 h. Mean±SD.

ATPase down-regulation in both human and experimental heart failure *in vivo* (*1*). Previously, we have reported alterations in cardiac function, in SR Ca^{2+} release and uptake functions, and in the expression of SR Ca^{2+} regulatory proteins (RyR and/or Ca^{2+}-ATPase) during the development of cardiac hypertrophy and heart failure in *in vivo* animal models (*3–6*). Our studies revealed that the nature of the alterations in SR function and SR Ca^{2+} regulatory proteins depended on the type of mechanical overload imposed and on the different duration of the heart disorder in these models. For instance, volume-overloaded hypertrophic rat hearts exhibited reduced SR functions and a decreased number of RyR, even in the hemodynamically compensatory (adaptive) stage (*3*). In contrast, in mildly pressure-overloaded rat hearts, cardiac hypertrophy was associated with an enhancement of the Ca^{2+} uptake and release functions of the SR and an up-regulated number of RyR during the early stage of the development of the hypertrophy (*4*). Interesting though these descriptive studies were, they did not identify the intracellular mechanisms responsible for the alterations in SR function and SR Ca^{2+} regulatory proteins induced by mechanical overload. Cultured neonatal rat cardiomyocytes have proven to be useful tools in our struggle to understand the cellular mechanisms involved in the regulation of SR Ca^{2+} regulatory proteins that occurs in response to mechanical factors. Although we have demonstrated that different types of cardiac-hypertrophy–inducing mechanical overload have different effects on SR Ca^{2+} regulatory proteins in *in vivo* animal models, it is currently unknown whether similar alterations are produced in response to extrinsic mechanical overload. Recently, Cadre *et al.* (*7*) reported that cyclic stretch caused a down-regulation of Ca^{2+}-transporter–gene expression in neonatal rat ventricular myocytes. Their results suggested that an *in vitro* model system should prove useful as a means of dissecting the cellular response during cardiac hypertrophy and heart failure *in vivo*.

The purpose of the present study was to determine whether, *in vitro*, an extrinsic mechanical overload (in the form of a high ambient pressure) would cause hypertrophy and an up-regulation of SR Ca^{2+} regulatory proteins (RyR and Ca^{2+}-ATPase) of the type previously reported by us in mildly hypertrophied rat hearts *in vivo*.

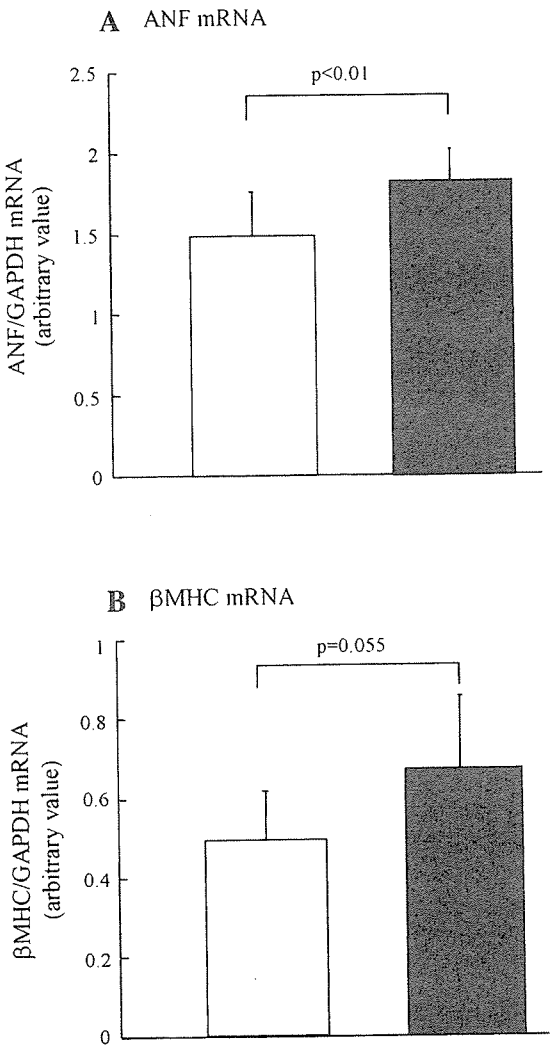

Fig. 1. *Expression levels of the mRNAs encoding atrial natriuretic factor (ANF) (A) and β-myosin heavy chain (βMHC) (B) in the cardiomyocytes either under atmospheric pressure conditions (APC, open bars) or under high pressure conditions (HPC, closed bars) for 24 h. Data are from 6 independent experiments in each group (mean±SD).*

Methods

Cell Culture

The animals used for this study were handled in accordance with the Guiding Principles in the Care and Use of Animals, as approved by the Animal Care Committee of Yamaguchi University Graduate School of Medicine. In addition, this investigation conforms with the Guide for the Care and Use of Laboratory Animals published by the US National Institutes of Health (NIH Publication No. 85-23, revised 1996). Primary cultures of neonatal rat cardiomyocytes were pre-

pared using the method originally described by Simpson *et al.* with minor modifications (*8*). Briefly, hearts from 1- or 2-day-old Wistar rats were minced, then dissociated with the aid of collagenase. After incubation of dispersed cells on 100-mm culture dishes (Falcon, Oxnard, USA) for 60 min at 37°C, non-attached viable cells were collected and seeded into 35-mm dishes (4×10^5 cells per dish). Cardiomyocytes were incubated in Leibovitz L-15 Medium (Worthington Biochemical Co., Lakewood, USA) supplemented with 10% fetal bovine serum and 0.1 mmol/l bromodeoxyuridine (BrDu) for the first 72 h. The serum was then replaced with 0.5% serum medium, and the cardiomyocytes were incubated for an additional 24 h. The cells were placed in the high pressure apparatus for 0–72 h. In certain experiments, we prepared cultures of almost pure monolayer cardiomyocytes with synchronous beating by the use of 0.1 mmol/l BrDu for the first 72 h after plating so as to inhibit fibroblast growth; this preferentially reduces the proportion of nonmyocytes as previously described (*9*). The percentage of cardiomyocytes was >95% at the start of the experiments.

Application of High Ambient Pressure

High ambient pressure was produced using the incubator and pressure-overloading apparatus previously developed in our laboratory (*10*). In brief, a small resealable acrylic chamber was designed to fit inside a standard incubator. This chamber had three openings: entrance and exit ports for compressed air and a hole for passing wires to both a pCO_2/pO_2 sensor (Microgas 7640; Kontron Instruments, Tokyo, Japan) and a pH sensor (Digitrapper Mk III; Synectics Medical, Stockholm, Sweden). A constant pressure chosen from within the range 0 to 1,013.3 hPa (0–760 mmHg) could be achieved by adding compressed air to the chamber to an appropriate extent. By changing the composition of the compressed air in advance, we could keep the pO_2 and pCO_2 concentrations of the air in the small chamber almost equal to those of atmospheric air (pO_2=205±0.7 hPa, pCO_2=49±0.7 hPa). In this study, cells were exposed to two conditions at 37°C: atmospheric pressure conditions (APC) and high pressure conditions (HPC). Measurement confirmed that the pH was identical (pH=7.4±0.05) in each of the mediums used under either of these two conditions. The HPC involved use of a pressure 200 mmHg above normal atmospheric pressure. This values was chosen because the use of a pressure 100 mmHg above normal atmospheric pressure caused no significant changes in neonatal cardiomyocytes and a pressure 300 mmHg above normal atmospheric pressure caused cell weakness (data not shown).

Measurement of Physiological and Morphological Characteristics

Physiological characteristics were monitored with a video-based edge-detection system (Ion Optix Co., Milton, USA) as previously reported (*11*). In brief, individual cardiomyocytes were placed on the stage of an inverted microscope (Eclipse TS100; Nikon, Tokyo, Japan) and displayed on a computer monitor by means of an Ion Optix MyoCam camera. Soft-edge-software (Ion Optix Co.) was then used to analyze the cardiomyocytes for cell length during shortening and relengthening. These physiological characteristics were measured for 72 h in each dish. The physiological performance of cardiomyocytes in 5 random fields (5 cells/field) was measured from 6 independent experiments.

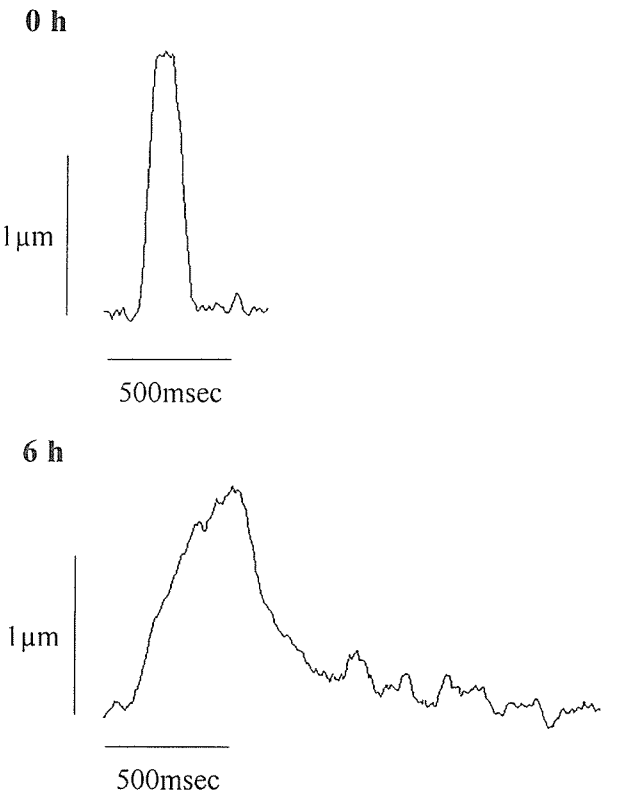

Fig. 2. *Effects of high pressure condition on physiological characteristics of cardiomyocytes. Examples of the cell contraction-relaxation in a cardiomyocyte exposed to high pressure for 0 h or 6 h are shown.*

For the measurement of cell size, cardiomyocytes were placed in 0.5% serum medium on a culture slide (BIOCOAT; Becton Dickinson Labware, Bedford, USA), cultured in the high ambient pressure apparatus under one of the pressure conditions for 0–72 h, then fixed with 10% formaldehyde solution in phosphate-buffered saline. Cell area was evaluated in haematoxylin-eosin preparations using a public image analysis application (NIH image). The cell size of cardiomyocytes in 10 random fields (50 cells/field) was measured from 6 independent experiments.

Table 2. Effects of Pressure-Overload on Physiological Characteristics of Cardiomyocytes

	T_{peak} (ms)	T_{70} (ms)	+dL/dt	−dL/dt
0 h	107±44	99±28	26.53±2.83	16.38±2.04
6 h	274±128$^{\#\#}$	165±6$^{\#}$	8.94±1.25$^{\#}$	12.29±6.23
24 h	121±61	170±80$^{\#}$	31.28±4.47	14.85±3.05
48 h	91±6	92±30	23.09±3.57	15.59±3.62
72 h	79±4	65±23	25.17±4.75	26.14±3.90$^{\#}$

T_{peak}, time to peak tension; T_{70}, time to 70% tension-regression; +dL/dt, maximal rate of shortening; −dL/dt, maximal rate of re-lengthening; $^{\#}p<0.05$, $^{\#\#}p<0.01$ *vs.* baseline (0 h). Mean±SD.

Western Blotting Analysis

Cells were lysed in protein lysis buffer (50 mmol/l Tris-HCl, pH 7.5, containing 150 mmol/l NaCl, 0.5% Nonidet P-40, 50 mmol/l NaF, 1 mmol/l Na_3VO_4, 1 mmol/l DTT, 1 mmol/l PMSF, 25 μg/ml leupeptin and 25 μg/ml aprotinin). Protein concentration was determined by a Bio-Rad Dc protein assay (Bio-Rad Laboratories, Hercules, USA). Immunoblot analysis was performed as previously described, with some modifications (*4*, *5*). Equal amounts of protein (80 μg/lane for RyR and 20 μg/lane for Ca^{2+}-ATPase) were electrophoretically separated on SDS-polyacrylamide gels and transferred to nitrocellulose membranes. The RyR and Ca^{2+}-ATPase protein bands were detected using monoclonal anti–ryanodine receptor antibody (Affinity Bioreagents, Inc., Golden, USA) and anti-SERCA2 ATPase antibody (Affinity Bioreagents, Inc.), respectively. The amount of protein recognized by the antibodies was quantified by means of an ECL immunoblotting detection system (Amersham, Bucks, UK), with the membrane being exposed to X-ray film. Quantitative densitometry of immunoblots was performed using a microcomputer imaging device (AE-6900M; ATTO, Tokyo, Japan).

RNA Preparation

Total cellular RNA was isolated from each frozen cell sample by the acid guanidinium thiocyanate/phenol/chloroform extraction method (*12*), then stored at −80°C.

Reverse Transcription and Polymerase Chain Reaction Amplification

The appropriate cDNAs were prepared using a Takara RNA PCR Kit (Takara, Tokyo, Japan), as previously described (*13*). The primers for the amplification of RyR, Ca^{2+}-ATPase, atrial natriuretic factor (ANF), β-myosin heavy chain (βMHC) and glyceraldehyde-3-phosphate dehydrogenase (GAPDH) were designed from published sequences. For the RyR, they were based on the following rat sequences (GenBank accession number U95157): at positions 455–483 (sense primer, 5′-GAGTCAGCATTCTGGAAGAAAATC ATAGC-3′) and 1191–1215 (antisense primer, 5′-GACATG GTCATATACCAGGCTAGGT-3′) (predicted length of the polymerase chain reaction [PCR] product, 761 bp). For the Ca^{2+}-ATPase, they were based on rat sequences (*14*) at positions 2951–2974 (sense primer, 5′-TGTCTGAAAACC AGTCCCTGCTGA-3′) and 3175–3199 (antisense primer, 5′-ATGGACCTCGGACGTTATGACCTCA-3′) (predicted length of the PCR product, 249 bp). For ANF, they were based on rat sequences (*15*) at positions 1–24 (sense primer, 5′-ATGGGCTCCTTCTCCATCACCAAG-3′) and 427–459 (antisense primer, 5′-TTATCTTCGGTACCGGAAGCT GTTGCAGCCTAG-3′) (predicted length of the PCR product, 459 bp). For βMHC, they were based on rat sequences (GenBank accession number X15939) at positions 5549–5569 (sense primer, 5′-ATCAAGGAGCTCACCTACCAG-3′) and 5864–5883 (antisense primer, 5′-GTC TGTTTCAAAGGCTCCAG-3′) (predicted length of the PCR product, 335 bp). For GAPDH, they were based on human sequences (*16*) at positions 102–125 (sense primer, 5′-CTTCATTGACCTCAACTACATGGT-3′) and 805–828 (antisense primer, 5′-CTCAGTGTAGCCCAGGATGCC CTT-3′) (predicted length of the PCR product, 726 bp).

Quantitation of PCR Products

The optimal number of amplification cycles needed to allow quantitation of RyR, Ca^{2+}-ATPase, ANF, βMHC and GAPDH gene PCR products was determined. The PCR products for each cycle were subjected to 5% polyacrylamide gel electrophoresis (PAGE) and autoradiography, then the associated radioactivity was measured using an imaging analyzer (model BAS-2000; Fuji Photo Film Co., Tokyo, Japan). The optimal number of cycles was found to be 25 for RyR, Ca^{2+}-ATPase, ANF, βMHC and GAPDH.

Assessment of the Expression of RyR, Ca^{2+}-ATPase, ANF and βMHC mRNAs

The relative radioactivity associated with RyR, Ca^{2+}-ATPase, ANF or βMHC PCR products in each sample was calculated by dividing the radioactivity associated with the RyR, Ca^{2+}-ATPase, ANF or βMHC PCR products by the radioactivity associated with the GAPDH gene product (internal control; amplified simultaneously). Each level of reverse transcription and PCR (RT-PCR) product was obtained from six indepen-

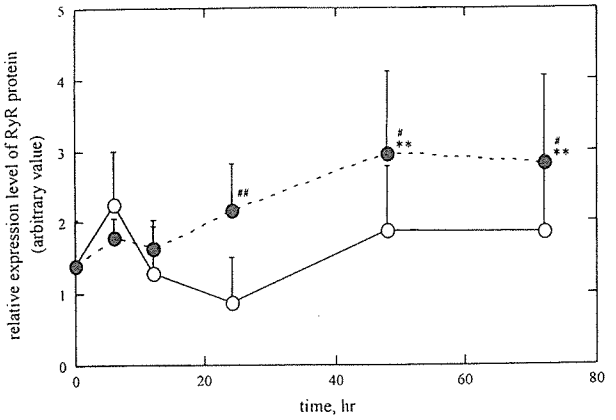

Fig. 3. *Time course of the effect of high ambient pressure on the relative expression level of RyR protein. Open circles, expression level under atmospheric pressure conditions (APC); closed circles, under high pressure conditions (HPC). Data are from 6 independent experiments in each group (mean±SD).* $^{**}p<0.01$ *vs. 0 h,* $^{\#}p<0.05$ *vs. APC,* $^{\#\#}p<0.01$ *vs. APC.*

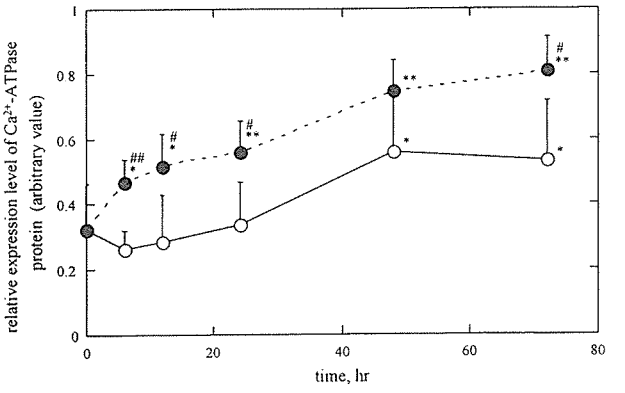

Fig. 4. *Time course of the effect of high ambient pressure on the relative expression level of* Ca^{2+}*-ATPase protein. Open circles, expression level under atmospheric pressure conditions (APC); closed circles, under high pressure conditions (HPC). Data are from 6 independent experiments in each group (mean±SD).* $^{*}p<0.05$ *vs. 0 h,* $^{**}p<0.01$ *vs. 0 h,* $^{\#}p<0.05$ *vs. APC,* $^{\#\#}p<0.01$ *vs. APC.*

dent experiments in each group. We used GAPDH as an internal control because the densitometric scores for the mRNAs did not differ between the groups of cells. Furthermore, this enzyme of the glycolytic pathway is constitutively expressed in most tissues and is the most widely accepted internal control in the molecular biology literature (*7*, *17*).

Statistical Analysis

All data are presented as the mean±SD. Comparisons between data were made using analysis of variance (ANOVA) followed by Fisher's test and Student's unpaired *t*-test. Differences were taken to be significant at $p<0.05$.

Results

Cardiomyocyte Characteristics

The application of high ambient pressure to neonatal cardiomyocytes produced myocyte hypertrophy. Tables 1 shows that the myocyte area was significantly greater in the HPC group than in the APC group at all timepoints. As seen in Fig. 1, at 24 h, the expression level of ANF mRNA in the HPC group (1.82±0.27) was significantly higher than that in the APC group (1.50±0.27, $p<0.01$). Moreover, ANF secretion in the HPC group (6.2±1.0 ng/ml) was significantly higher than in the APC group (3.8±0.2 ng/ml, $p<0.01$). The expression level of βMHC mRNA in the HPC group (0.67±0.18) was higher than that in the APC group (0.50±0.12), but the difference did not reach the level of statistical significance ($p=0.055$). There was no significant difference in the relative spontaneous beating rate, which was calculated by dividing the beating rate at each timepoint by the beating rate before the exposure (at 0 h), between the APC and HPC groups (data not shown). Both the example (Fig. 2) and the summary data (Table 2) show the physiological characteristics of cardiomyocytes exposed to HPC. After 6 h exposure, HPC caused a transient impairment of contraction-relaxation performances, but the contraction properties of cardiomyocytes returned to the baseline level within 24 h. Interestingly, after 72 h the rate of cell re-lengthening ($-dL/dt$) increased significantly compared with that at baseline. In the APC group, there were no significant differences in the physiological characteristics of cardiomyocytes over the 72-h culture period.

Analysis of the Expression Levels of RyR and Ca^{2+}-ATPase Proteins

The expression level of RyR protein (Fig. 3) in the HPC group gradually increased after the exposure began and, at 24 h, the expression level was significantly greater than in the APC group (2.16±0.67 *vs.* 0.88±0.62, $p<0.05$). Moreover, at 48 h, the expression level under HPC (2.94±1.17) was significantly higher than that at 0 h in the same group (1.41±0.63, $p<0.05$). The up-regulation continued for 72 h under HPC. In contrast, although there was a slight but not significant decrease in the expression of RyR protein at 24 h, there was no significant change in the expression level of RyR protein under APC over the 72 h of the experiment. Interestingly, in the case of Ca^{2+}-ATPase protein (Fig. 4), the expression level gradually increased not only under HPC, but also under APC. Under HPC, the expression level of Ca^{2+}-ATPase protein at 6 h was significantly greater than that under APC at the same timepoint (0.47±0.07 *vs.* 0.26±0.06, $p<0.01$) and significantly greater than at time 0 h (0.33±0.14, $p<0.05$), and the

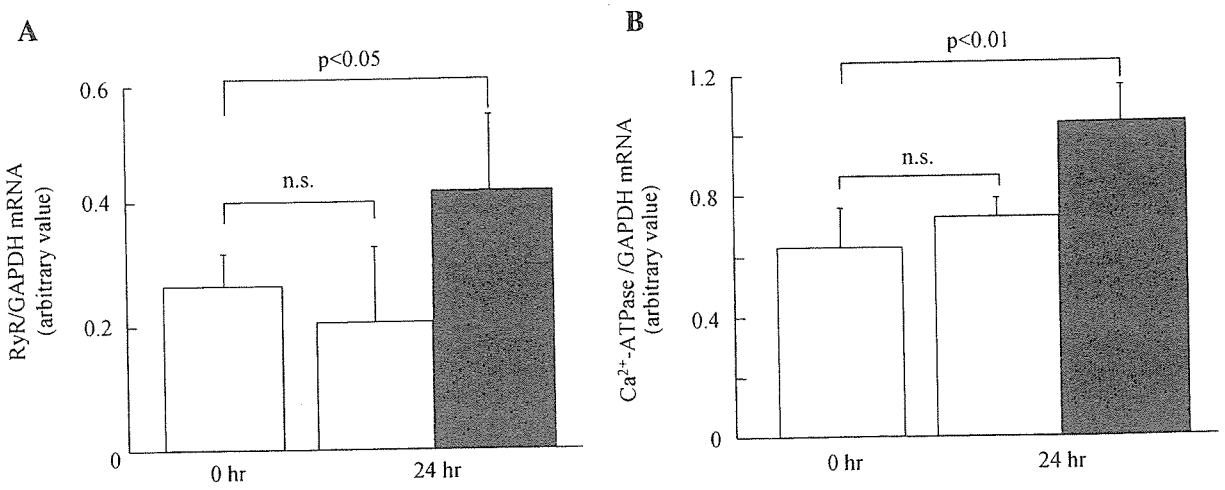

Fig. 5. *Expression levels of the mRNAs encoding RyR (A) and Ca^{2+}-ATPase (B) after high pressure exposure. Neonatal cardiac myocyte cultures were maintained under atmospheric pressure conditions (APC, open bars) or high pressure conditions (HPC, closed bar). Under HPC, the relative expression levels of RyR and Ca^{2+}-ATPase mRNA were significantly increased, but under APC there was no significant difference in the expression levels of either mRNA between 0 h and 24 h. Data are the mean±SD from 6 independent cell isolations.*

up-regulation persisted until 72 h after the start. Under APC, the expression of Ca^{2+}-ATPase protein was significantly greater at 48 h than at 0 h (0.56±0.18 *vs.* 0.33±0.14, $p<0.05$), and the increase persisted until the end of the experiment at 72 h.

Analysis of the Expression Levels of the mRNAs for RyR and Ca^{2+}-ATPase

As indicated in Fig. 5, high ambient pressure significantly increased the relative expression levels of the mRNAs encoding RyR and Ca^{2+}-ATPase. These increased levels persisted until 72 h of exposure (data not shown). Under HPC, the relative expression level of RyR mRNA was significantly increased after 24 h of exposure (from 0.269±0.056 to 0.414±0.123; $p<0.05$) (Fig. 5A) and the relative expression level of Ca^{2+}-ATPase mRNA was also significantly increased after 24 h of exposure (from 0.635±0.129 to 1.030±0.121; $p<0.01$) (Fig. 5B). Under APC, there was no significant difference in the expression levels of either of the mRNAs between 0 h and 24 h (at 24 h: 0.233±0.102 for RyR mRNA and 0.735±0.060 for Ca^{2+}-ATPase mRNA). Interestingly, at 24 h the relative expression level of the Ca^{2+}-ATPase mRNA under APC (0.735±0.060) tended to show an increase, although the difference was not significant.

Discussion

The major findings of the present study were as follows: 1) we showed that an *in vitro* high pressure-overload model system for cultured cardiac myocytes can be used to investigate alterations in SR Ca^{2+} regulatory proteins during the development of hypertrophy; 2) both RyR and Ca^{2+}-ATPase expressions were up-regulated in hypertrophied cardiac myocytes subjected to a high ambient pressure, contributing at least in part to the maintenance of contraction-relaxation characteristics in cardiac myocytes. To our knowledge, although there have been many investigations of the alterations in cardiac SR Ca^{2+} regulatory proteins associated with stretch-induced myocyte hypertrophy *in vitro*, this is the first investigation in which changes in these proteins have been evaluated under high ambient pressure conditions in cultured cardiac myocytes. Due to the complex *in vivo* physiology of cardiac hypertrophy, it is very difficult to define the signaling mechanisms responsible for the alterations in cardiac myocyte gene expression that in turn may contribute to the pathogenesis of this disorder. Cultured neonatal rat myocytes have been a useful model for clarifying the mechanisms involved in the regulation of SR Ca^{2+} regulatory proteins that occurs in response to mechanical factors.

As described in Introduction, recent studies have demonstrated that the alterations occurring in SR Ca^{2+} regulatory proteins during cardiac hypertrophy depend on the type of mechanical overload imposed (*1*, *3–6*). The mechanisms underlying these alterations are still unknown and it is unclear whether they are a direct effect or a secondary effect resulting from the imposition of mechanical overload on cardiac myocytes. In a series of *in vitro* studies, the stretching of cultured cardiac myocytes obtained from neonatal rats was shown to induce severe hypertrophy and to stimulate both protein synthesis and specific gene expression (*18*, *19*). Cadre *et al.* (*7*) reported that cyclic stretch induced hypertrophy of neonatal rat ventricular myocytes and significantly down-regulated the expressions of RyR and Ca^{2+}-ATPase (at both the mRNA and

protein levels). Such down-regulation is a characteristic result of volume-overload of the rat heart *in vivo*, as demonstrated in our previous report (*3*). The present study was designed to assess the *in vitro* effects of high ambient pressure, not of stretch-overload, on cultured neonatal cardiac myocytes and to determine whether such high ambient pressure might affect the expression of SR Ca^{2+} regulatory proteins (RyR and Ca^{2+}-ATPase) during the development of hypertrophy. Interestingly, we showed that high ambient pressure induced myocyte hypertrophy and an up-regulation of RyR and Ca^{2+}-ATPase (at both the mRNA and protein levels), effects that are characteristic of a mild pressure-overloading of the rat heart *in vivo* (*4*, *20*).

Mechanical stimuli cause a rapid change in gene expression in cardiac myocytes (*18*, *19*). Many mechanosensitive ion channels and exchangers play critical roles in stretch-induced myocyte hypertrophy (*21*). Linear stretch of cardiac myocytes *in vitro* causes a transcriptional activation of immediate-early genes, followed by an induction of the fetal genes for atrial natriuretic factor, skeletal α-actin and β-myosin heavy chain (*19*). Moreover, recent evidence indicates that mechanical stretch has a close relationship with autocrine-paracrine growth factors in the heart, such as those of the tissue renin-angiotensin system (*18*, *22*). At present, it is not clear why the expression of RyR and Ca^{2+}-ATPase proteins and genes show either an increase or a decrease depending on the type of mechanical overload. In the case of the Ca^{2+}-ATPase gene, Fisher *et al.* (*23*) demonstrated that the promoter region, which extends from the transcriptional start site to −284, produces enhanced transcriptional activity, whereas the region from −1100 to −284 exerts a negative transcriptional effect in the adult myocardium. Arai *et al.* (*20*) speculated in their report that the interaction between the *trans*-acting factors associated with hemodynamic overload and these promoter regions may be responsible for the up- or down-regulation of the Ca^{2+}-ATPase gene. Although knowledge of the cellular and molecular mechanisms underlying stretch-induced hypertrophy has increased considerably in recent years, the mechanisms underlying high ambient pressure-induced hypertrophy are still unclear and demand further investigation.

Interestingly, in our cultured neonatal rat cardiac myocytes the level of Ca^{2+}-ATPase protein gradually increased (unlike that of RyR protein) not only under HPC, but also under APC. In our experiments, we prepared cardiomyocytes from 1- or 2-day-old rat hearts and cultured then up to 7 days. Shiojima *et al.* (*24*) examined developmental changes in Ca^{2+}-ATPase and reported that the expression of Ca^{2+}-ATPase mRNA was significantly lower than the post-natal level during the early embryonic period, but increased dramatically starting 2 days before birth. These data and ours indicate that the expression of Ca^{2+}-ATPase is regulated both by hemodynamic load and development stage.

We should point out some limitations of the present study. First, in this study, a pressure of 200 mmHg was necessary to induce significant hypertrophy of the cardiomyocytes. This 200 mmHg was provided as a compressive pressure or ambient pressure onto the monolayer cells. Some may object that this value is far beyond the pressure in a real clinical setting, in which mean intraventricular pressure is usually less than 150 mmHg, even if a ventricular pressure overload exists. However, we do not know what the 200 mmHg of pressure used in our *in vitro* model corresponds to in terms of actual mean intraventricular cavity pressure, because the accurate values for the compressive pressure or compressive stress for individual cells have not been measured *in vivo*. Our study is the first report of the effect of excessive ambient pressure on myocardial cell hypertrophy, so further examination will be needed to assess the clinical applicability of our results. Second, we could not perform a functional examination of the SR, because of the difficulty of performing such studies on cultured cardiac myocytes and because the amount of SR that can be obtained from cultured cells is limited. Third, we need to monitor intracellular Ca^{2+} transients. We speculated that the increases in RyR and Ca^{2+}-ATPase proteins could cause changes in the intracellular Ca^{2+} homeostasis, but we have not directly shown that the increase in these proteins has "functional" consequences for intracellular Ca^{2+} transients. Clearly, examination of the intracellular Ca^{2+} transients of pressure-overloaded hypertrophied myocytes would be of great interest. Finally, the contraction-relaxation characteristics of cardiac myocytes subjected to high ambient pressure were regulated not only by SR Ca^{2+} regulatory proteins, but also by several other factors—*e.g.*, myofilament characteristics and/or neurohumoral factors produced by cardiomyocytes themselves. Further experimental studies will be needed to clarify the contributions made by each of these factors in this *in vitro* high pressure model.

In conclusion, our results indicate that high ambient pressure induces hypertrophy in neonatal rat cardiac myocytes and causes up-regulation of RyR and Ca^{2+}-ATPase in cultured cardiac myocytes. The results of the present study are compatible with the hypothesis that in the mechanically overloaded heart, genes encoding proteins involved in SR Ca^{2+} regulation are up- or down-regulated in a manner dependent on the type of load. The present *in vitro* high pressure model may prove useful, like stretch-overload models, for the investigation of the intracellular Ca^{2+} regulatory pathways responsible for the development of cardiac hypertrophy *in vivo*.

References

1. Arai M, Matsui H, Periasamy M: Sarcoplasmic reticulum gene expression in cardiac hypertrophy and heart failure. *Circ Res* 1994; **74**: 555–564.
2. Diamond JA, Phillips RA: Hypertensive heart disease. *Hypertens Res* 2005; **28**: 191–200.
3. Hisamatsu Y, Ohkusa T, Kihara Y, *et al*: Early changes in the functions of cardiac sarcoplasmic reticulum in volume-overloaded cardiac hypertrophy in rats. *J Mol Cell Cardiol* 1997; **29**: 1097–1109.

4. Ohkusa T, Hisamatsu Y, Yano M, *et al*: Altered cardiac mechanism and sarcoplasmic reticulum function in pressure overload–induced cardiac hypertrophy in rats. *J Mol Cell Cardiol* 1997; **29**: 45–54.
5. Ueyama T, Ohkusa T, Hisamatsu Y, *et al*: Alteration in cardiac SR Ca^{2+}-release channels during development of heart failure in cardiomyopathic hamsters. *Am J Physiol* 1998; **274**: H1–H7.
6. Ueyama T, Ohkusa T, Yano M, Matsuzaki M: Growth hormone preserves cardiac sarcoplasmic reticulum Ca^{2+} release channels (ryanodine receptors) and enhances cardiac function in cardiomyopathic hamsters. *Cardiovasc Res* 1998; **40**: 64–73.
7. Cadre BM, Qi M, Eble DM, *et al*: Cyclic stretch down-regulates calcium transport gene expression in neonatal rat ventricular myocytes. *J Moll Cell Cardiol* 1998; **30**: 2247–2259.
8. Simpson P, McGrath A, Savon S: Myocyte hypertrophy in neonatal rat heart cultures and its regulation by serum and by catecholamines. *Circ Res* 1982; **51**: 787–810.
9. Ing DJ, Zang J, Dzau V: Modulation of cytokine-induced cardiac myocyte apoptosis by nitric oxide, Bak, and Bcl-x. *Circ Res* 1999; **84**: 21–33.
10. Kawata Y, Fujii Z, Sakumura T, *et al*: High pressure conditions promote the proliferation of rat cultured mesangial cells *in vitro*. *Biochim Biophys Acta* 1998; **1401**: 195–202.
11. Mizukami Y, Iwamatsu A, Kimura M, *et al*: ERK1/2 regulates intracellular ATP levels through alpha-enolase expression in cardiomyocytes exposed to ischemic hypoxia and reoxygenation. *J Biol Chem* 2004; **279**: 50120–50131.
12. Mullis K, Faloona F, Scharf S, *et al*: Specific enzymatic purification of DNA *in vitro*; the polymerase chain reaction. *Cold Spring Harb Symp Quant Biol* 1986; **51**: 263–273.
13. Ohkusa T, Ueyama T, Yamada J, *et al*: Alterations in cardiac sarcoplasmic reticulum Ca^{2+} regulatory proteins in the atrial tissue of patients with chronic atrial fibrillation. *J Am Coll Cardiol* 1999; **34**: 255–263.
14. Lompre AM, de la Bastie D, Boheler KR, Schwartz K: Characterization and expression of the rat heart sarcoplasmic reticulum Ca^{2+}-ATPase mRNA. *FEBS Lett* 1989; **249**: 35–41.
15. Maki M, Takayanagi R, Misono KS, Pandy KN, Tibbetts C, Inagami T: Structure of rat atrial natriuretic factor precursor deduced from cDNA sequence. *Nature* 1984; **309**: 722–724, 1984.
16. Tso JY, Sun X-H, Kao T, Reece KS, Wu R: Isolation and characterization of rat and human glyceraldehyde-3-phosphate dehydrogenase cDNAs: genomic complexity and molecular evolution of the gene. *Nucleic Acids Res* 1985; **13**: 2485–2502.
17. Takahashi T, Allen PD, Izumo S: Expression of A-, B-, and C-type natriuretic peptide gene in failing and developing human ventricles: correlation with expression of the Ca^{2+}-ATPase gene. *Circ Res* 1992; **71**: 9–17.
18. Komuro I, Kaida T, Shibazaki Y, *et al*: Stretching cardiac myocytes stimulates protooncogene expression. *J Biol Chem* 1990; **265**: 3595–3598.
19. Komuro I, Katoh Y, Kaida T, *et al*: Mechanical loading stimulates cell hypertrophy and specific gene expression in cultured rat cardiac myocytes. *J Biol Chem* 1991; **266**: 1265–1268.
20. Arai M, Suzuki T, Nagai R: Sarcoplasmic reticulum genes are upregulated in mild cardiac hypertrophy but downregulated in severe cardiac hypertrophy induced by pressure overload. *J Moll Cell Cardiol* 1996; **28**: 1583–1590.
21. Yamazaki T, Komuro I, Kudoh S, *et al*: Role of ion channels and exchangers in mechanical stretch–induced cardiomyocyte hypertrophy. *Circ Res* 1998; **82**: 430–437.
22. Sadoshima J, Jahn L, Takahashi T, Kulik TJ, Izumo S: Molecular characterization of the stretch-induced adaptation of cultured cardiac cells: an *in vitro* model of load-induced cardiac hypertrophy. *J Biol Chem* 1992; **267**: 10551–10560.
23. Fisher SA, Buttrick PM, Sukovich D, Periasamy M: Characterization of promoter elements of the rabbit cardiac sarcoplasmic reticulum Ca^{2+}-ATPase gene required for expression in cardiac muscle cells. *Circ Res* 1993; **73**: 622–628.
24. Shiojima I, Komuro I, Yamazaki T, Nagai R, Yazaki Y: Molecular aspects of the control of myocardial relaxation, in Lorell BH & Grossman W (eds): Diastolic Relaxation of the Heart. Norwell, Kluwer Academic Publishers, 1994, pp 25–32.

Circ J 2007; **71:** 57–62

Different Effect of the Pure Na^+ Channel-Blocker Pilsicainide on the ST-Segment Response in the Right Precordial Leads in Patients With Normal Left Ventricular Function

Takeshi Ueyama, MD; Akihiko Shimizu, MD*; Toshihiko Yamagata, MD**; Masahiro Esato, MD; Masato Ohmura, MD; Yasuhiro Yoshiga, MD; Masashi Kanemoto, MD; Ryousuke Kametani, MD; Akira Sawa, MD; Shinsuke Suzuki, MD; Naoki Sugi, MD; Masunori Matsuzaki, MD

Background The response of the ST-segment in the right precordial leads to Na^+ channel blockers in patients without structural heart disease and a typical Brugada-type ECG has not been fully elucidated.
Methods and Results A pilsicainide challenge test was performed in 161 patients and according to recently established ECG criteria and an organized computer algorithm, the ST morphology was classified and the maximum increase in the J wave amplitude (maxΔJ) from the standard and high right precordial leads V_{1-3} was examined. Before the test, subjects exhibiting type 1 ECG in the standard leads were excluded. After administering pilsicainide, type 1 ECGs in the standard leads were observed in 31 cases and a maxΔJ of $\geq 200\mu V$ was observed in 29 cases (23 type 1, 2 type 2/3 and 4 normal ECGs). In the additional higher right precordial leads, type 1 ECGs were observed in 55 cases and a maxΔJ of $\geq 200\mu V$ was observed in 45 cases (42 type 1 and 3 type 2/3 ECGs).
Conclusions A maxΔJ $\geq 200\mu V$ induced by pilsicainide, including that measured in the high right precordial leads, was associated with a change mainly to a type 1 ECG. (*Circ J* 2007; **71:** 57–62)

Key Words: Brugada syndrome; Brugada-type ECG; Drug challenge test; Pilsicainide; ST-segment

Although Na^+-channel blockers are widely used for various arrhythmias in clinical practice, they can unmask the Brugada-type ECG and further induce elevation of the ST-segment, which can sometimes lead to ventricular tachyarrhythmias in patients with Brugada syndrome (BS).[1–3] The response of the ST-segment to Na^+-channel blockers in structurally normal hearts has seldom been discussed because the main effects of Na^+-channel blockers on the ECG are QRS and QT prolongation. Recently, drug challenge tests using Na^+-channel blockers have generally become accepted as a useful method for diagnosing BS, as described in the consensus report endorsed by the Heart Rhythm Society and the European Heart Rhythm Association.[4,5] However, there is still controversy over whether or not these drugs are specific for BS,[6,7] and the prevalence of similar drug responses with BS in structurally normal hearts is not well known.

The use of the Na^+-channel-blocker challenge test using ajmaline, flecainide or propafenone has been recently reported in a relatively large patient population.[8–10] Ajmaline is frequently used in drug challenge tests in European countries, but is infrequently used in Japan. Flecainide and propafenone not only have Na^+-channel-blocking effects, but also have K^+-channel blocking and β-blocking effects.[11] Pilsicainide has pure and strong Na^+-channel-blocking effects and is the drug most often used in Japan for clinical drug challenge tests,[12] therefore we used it in the present study to assess the influence of pilsicainide on the surface ECG not only in patients suspected of BS, but also in patients in whom Na^+-channel blockers would be used.

(Received January 23, 2006; revised manuscript received September 6, 2006; accepted October 25, 2006)
*Division of Cardiovascular Medicine, Department of Medical Bioregulation, *Faculty of Health Sciences, Yamaguchi University Graduate School of Medicine, Ube and **Department of Cardiology, Yamaguchi Grand Medical Center, Hofu, Japan*
Mailing address: Takeshi Ueyama, MD, Division of Cardiovascular Medicine, Department of Medical Bioregulation, Yamaguchi University Graduate School of Medicine, 1-1-1 Minamikogushi, Ube 755-8505, Japan. E-mail: ueyama@yamaguchi-u.ac.jp

Methods

Subjects

We prospectively studied 161 consecutive patients who had normal left ventricular function with no evidence of typical Brugada signs on their baseline ECG during hospitalization and who consented to a Na^+-channel-blocker challenge test during the period from January 2002 to August 2005. There were 135 males and 26 females with a mean age of 53±15 years. The pilsicainide test was performed in symptomatic (n=95, 79 males, 52±16 years) and asymptomatic (n=66, 56 males, 54±14 years) patients. The symptomatic patients had a history of documented arrhythmias other than ventricular tachycardia (VT) or ventricular fibrillation (VF), or episodes related to brain ischemia such as syncope or fainting, but no documented arrhythmias at that time. In the present study, VT was defined as more than ventricular triplets. The asymptomatic patients were selected from a healthy population with documented ECG abnormalities suspected of being Brugada-type or Brugada-like, other than ones with the coved-type ST elevation or with arrhythmias such as ventricular premature contractions (VPCs) or atrial premature contractions diagnosed by yearly health check-ups (Table 1).

Three types of repolarization pattern were recognized

Table 1 Clinical Characteristics of the Subjects

Clinical presentation	*No. of patients*
Symptomatic patients	*95*
Symptom related arrhythmias	*57*
Syncope or fainting	*38*
Asymptomatic patients	*66*
ECG abnormalities with a Brugada sign	*58*
*Arrhythmias**	*8*

**: 1 atrial premature contractions, 6 ventricular premature contractions and 1 paroxysmal supraventricular tachycardia.*

and defined as types 1, 2 and 3 according to the Heart Rhythm Society and the European Heart Rhythm Association[4] We used these ECG criteria and excluded subjects exhibiting type 1 ECGs in the standard leads in the control state. We also excluded patients with VT (≥triplets), or a family history of BS or sudden unexpected death. All cases then underwent echocardiography with careful attention paid to any right ventricular (RV) enlargement and/or wall motion abnormalities and were also checked for conditions and agents that may lead to ST-segment elevation[4] Therefore, patients with organic heart disease or other factors that may have influenced ST-segment elevation were excluded.

All patients gave written informed consent to participate in the study, which was approved by the Institutional Clinical Research and Ethics Committee.

Na^+-Channel-Blocker Challenge Test

We performed a Na^+-channel-blocker challenge test using pilsicainide, a so-called pure Na^+-channel blocker, in a room with a defibrillator and life support facilities. Pilsicainide was administrated intravenously at a speed of 0.1 $mg \cdot kg^{-1} \cdot min^{-1}$ over 10 min (total 1 mg/kg) with continuous ECG and non-invasive blood pressure monitoring. During drug administration, we monitored the ECG using the standard 12 leads, but after performing 96 tests, we began monitoring not only the standard right precordial leads V_{1-3}, but also those recorded from 1 intercostal space (ICS) higher than the right precordial leads using the V_{4-6} electrodes, because in several cases we found marked ST elevation after the pilsicainide test in the higher right precordial leads only. Drug administration was immediately stopped when ST elevation (>0.5 mV), extensive QRS prolongation, unfavorable symptoms and/or frequent ventricular arrhythmias were observed. In this study, the test was considered positive if the abnormal coved-type ECG pattern (type 1 ECG) appeared in more than 1 right precordial lead.

Electrocardiography

Before and after the administration of pilsicainide, we recorded the standard 12-lead ECG (ECG-9322, Nihon Kohden Corp, Tokyo, Japan). The J wave amplitude (STJ; μV) was analyzed by an organized computer algorithm (ECAPS 12C, Nihon Kohden). In the ECAPS 12C, the terminal point of the QRS (J point) was defined as the offset point of the QRS waveform determined from the averaged QRS waveforms from the 12 leads. After the drug test, we calculated the increase in the STJ (ΔJ) in each of the right precordial leads (V_{1-3}). The maximum increase in the STJ (maxΔJ) was defined as the maximum value of ΔJ of the 3 leads. Based on the ECG criteria, we defined it as either a "Brugada-type" type 1 ECG (coved type with an STJ ≥200μV), or "suspect Brugada-type" type 2/3 ECG (saddle-back type with an STJ ≥200μV), and these were reviewed by 2 independent cardiologists. The other ECGs without these criteria were defined as "normal", including Brugada "like" ECGs of either the coved or saddle-back type with an STJ <200μV and non-specific ST elevation with an STJ ≥200μV. As described in the primary consensus report[4] an increase in the J wave amplitude of greater than 200μV was also considered a significant diagnostic value, and we assessed the prevalence of ST morphology and maxΔJ, with a cutoff point defined as 200μV in the high right precordial leads during Na^+-channel blocker administration.

Table 2 The Value of the J Wave Amplitude in the Right Precordial Leads and QRS Width Before and After Pilsicainide

	Before	*After*
V_1 (μV)	*72±48*	*102±111*
V_2 (μV)	*153±70*	*259±155**
V_3 (μV)	*128±65*	*204±95**
1 h V_1 (μV)	*60±53*	*90±118*
1 h V_2 (μV)	*132±87*	*236±193**
1 h V_3 (μV)	*124±66*	*214±116**
2 h V_1 (μV)	*35±47*	*58±104*
2 h V_2 (μV)	*82±67*	*151±152**
2 h V_3 (μV)	*106±63*	*191±131**
QRS (ms)	*96±11*	*120±12**

*vs before: *p<0.001.*
Before, before the pilsicainide administration; after, after the pilsicainide administration; V_n, *right precordial lead* V_n *(n=1–3);* 1 hV_n, *right precordial lead 1 intercostal space above lead* V_n *(n=1–3);* 2 hV_n, *right precordial lead 2 intercostal spaces above lead* V_n *(n=1–3).*

ECG From the High Right Precordium

To evaluate the ST-segment recorded from the high right precordium in all cases, we moved the 3 leads 1 or 2 ICS higher after making baseline recordings from the standard leads before and after pilsicainide. From all the ECGs recorded, including those from the higher placement of leads, we assessed the maxΔJ and ST morphology.

Statistical Analysis

Data are given as the mean±SD. The ECG data were analyzed by paired t-test. The chi-square test for independence was used for comparisons of the prevalence of a type 1 ECG after giving pilsicainide in 2 groups divided by a cutoff point of 200μV for the maxΔJ. A value of $p<0.05$ was considered statistically significant.

Results

Pilsicainide Dose and Effect on J Wave Amplitude and QRS Width

In the 161 cases, the administration of pilsicainide was stopped in 21 when the ST junction in the right precordial leads became elevated by more than 0.5 mV and/or the number of VPCs and couplets increased. The mean dose was 0.97 mg/kg. Severe complications, such as VT or VF, did not occur.

Pilsicainide increased the STJ in each lead, and a significant increase in leads V_2 and V_3 recorded from both the standard and higher positions was especially noted. The QRS width was significantly prolonged in all patients (Table 2).

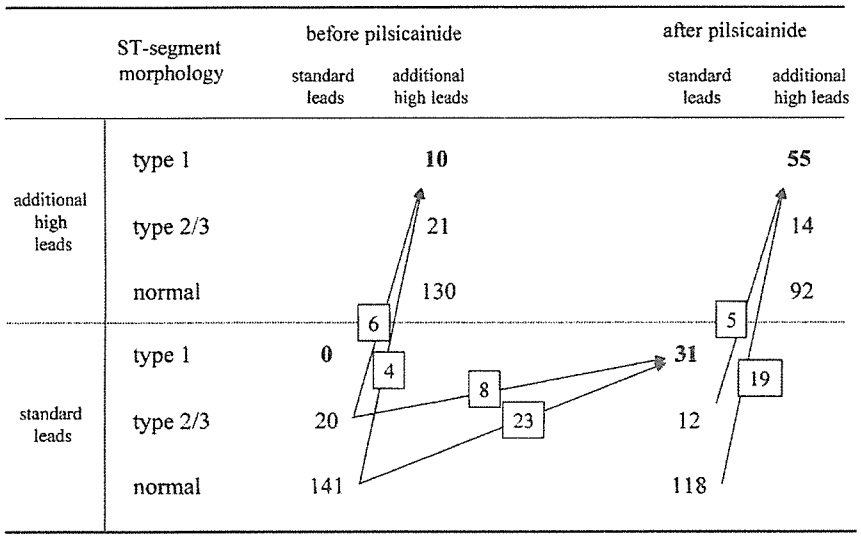

Fig 1. Prevalence of the ST-segment morphology before and after the pilsicainide test. The arrows indicate the change in the morphology of the ST-segment with pilsicainide. Type 1, coved type ST elevation, type 2/3, type 2 and 3 saddle-back type ST elevation adopted by the Study Group on the Molecular Basis of Arrhythmias of the European Society of Cardiology[4]

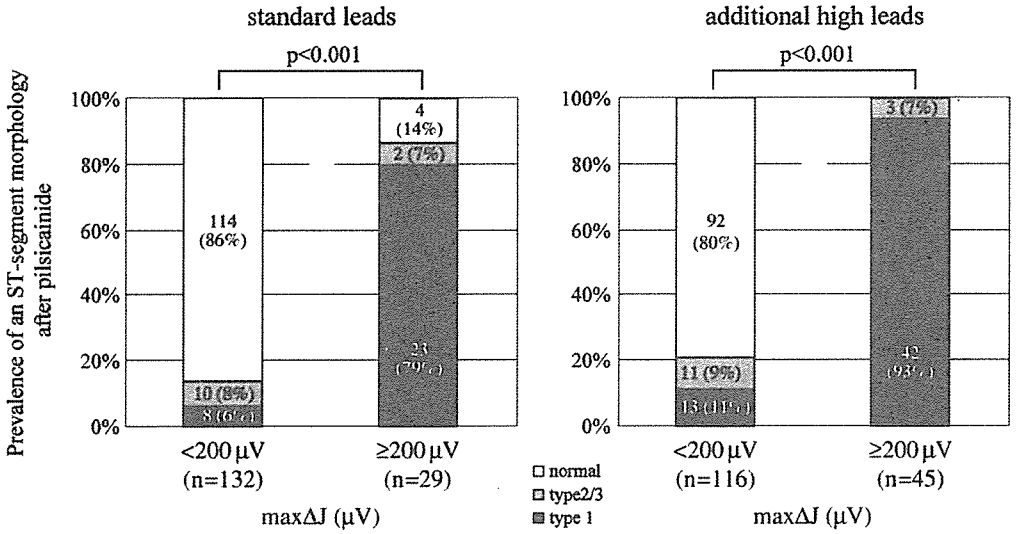

Fig 2. Prevalence of the ST-segment morphology in relation to the maxΔJ. (Left) Proportion of each ST-segment morphology in the standard leads after pilsicainide in the 2 groups divided by a cut-off point of 200μV for the maxΔJ. (Right) Proportion of each ST-segment morphology in the high right precordial leads. (■) Type 1 ECG after pilsicainide; (▨) type 2/3 ECG after pilsicainide; (□) normal ECG after pilsicainide.

Prevalence of the Brugada-Type ECG Before and After Drug Challenge Test

Before the administration of pilsicainide, suspicious Brugada-type ECGs (type 2/3) were observed in 20 cases (12%). After the administration of pilsicainide, Brugada-type ECGs (type 1) were observed in 31 cases (19%), which at baseline were type 2/3 ECG in 8 cases and normal ECG in 23 cases.

Including the recordings from the higher placement of the leads, in 10 cases a type 1 ECG before pilsicainide was documented, which in the baseline standard leads had been a type 2/3 ECG in 6 cases and normal ECG in 4 cases. After pilsicainide, 24 more cases had a documented type 1 ECG, which in the standard leads was a type 2/3 ECG in 5 cases and normal ECG in 19 cases (Fig 1).

Distribution of the Maximum Increase in the STJ

In the standard ECG leads, a maxΔJ ≥200μV was observed in 29 cases (type 1 ECG in 23 cases, type 2/3 ECG in 2 cases, normal ECG in 4 cases) after pilsicainide (Fig 2). In 5 of 6 cases that did not exhibit a type 1 ECG, a type 1 ECG could be detected when the right precordial leads were moved higher.

When the high right precordial leads were included, 16 more cases, which had a maxΔJ <200μV in the standard leads, had a maxΔJ ≥200μV. In 42 of 45 cases with a maxΔJ ≥200μV in which the higher leads were included, the ECG exhibited a type 1 ECG. In contrast, the maxΔJ in all the patients with a normal ECG after the pilsicainide test, even when recording from the higher leads, did not exceed 200μV. The prevalence of ST-segment morphology with a maxΔJ greater than and less than 200μV significantly differed for both recording methods (Fig 2). Further, there were no normal ECGs with a maxΔJ ≥200μV in the analysis of the additional higher leads (Fig 2). A representative case of a type 1 ECG in only the higher leads after pilsicainide is shown in Fig 3. Each value of the maxΔJ for each type of ST-segment morphology after pilsicainide,

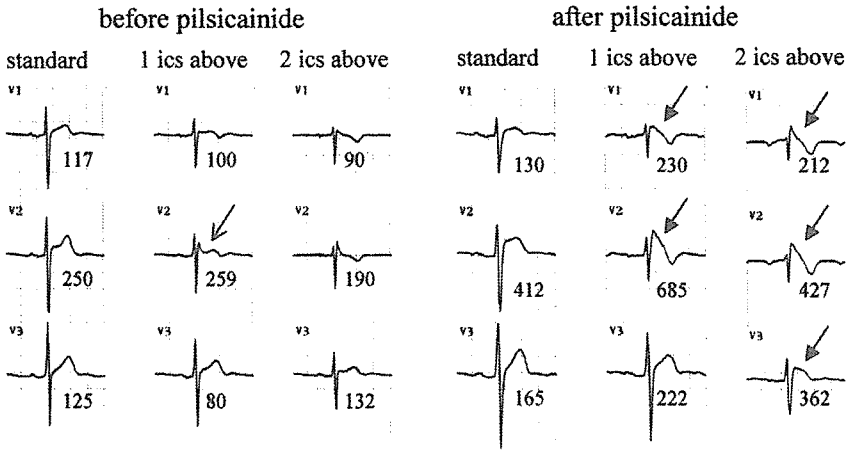

Fig 3. Representative case of type 1 ECG after pilsicainide recorded from the upper intercostal leads. A 29 year-old male, who had suffered from unexplained syncope, had ECGs recorded from the right precordial leads and 1 and 2 intercostal spaces (ICS) above leads V_{1-3}. Before pilsicainide, non-specific ST elevation was observed in V_2 and a type 2 ECG appeared in a recording from 1 ICS above V_2 (arrow). After pilsicainide (1 mg/kg), type 1 ECGs were unmasked only in the high right precordial leads (arrowhead). The number shows the J wave amplitude (μV).

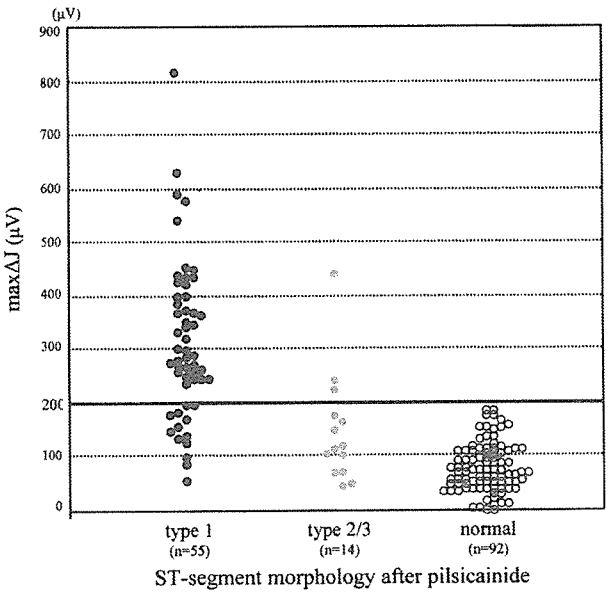

Fig 4. Scatter plot of the maxΔJ in relation to the ST-segment morphology after pilsicainide administration when recording from the higher leads. The panel shows the scatter plot of the maxΔJ analyzed in the high right precordial leads. (●) Type 1 ECG after pilsicainide; (◍) type 2/3 ECG after pilsicainide; (○) normal ECG after pilsicainide. The straight bold line in the graph represents a maxΔJ of 200μV and the distribution of the normal ECGs (○) after administering pilsicainide is shown underneath. In contrast, the ST-segment morphology of the distribution above the line contains all type 1 ECGs (●), except for 3 type 2/3 ECGs (◍). The line shows the cutoff that divides the distribution of the normal ECGs after the pilsicainide administration, and the cutoff value for the maxΔJ is 200μV.

including those for the additional higher leads, is plotted in Fig 4. Note that there were no patients with a maxΔJ $\geq$200μV in the normal ECGs after pilsicainide. In Fig 4 200μV maxΔJ represents the cutoff line and value that was used to divide the distribution of the normal ECGs from abnormal ECGs after pilsicainide.

Discussion

In the present study, we assessed the prevalence of a Brugada-type (type 1) ECG and the increase in the J wave amplitude in the right precordial leads, including higher placement of the leads, in order to evaluate the effects of pilsicainide on the ST-segment in the ECGs not exhibiting a type 1 ECG in the standard leads during the control state. We found that the prevalence of a type 1 ECG after pilsicainide was 19% and the prevalence of a maxΔJ $\geq$200μV after the test was 18% in the standard leads. By recording from the high right precordial leads, the prevalence of a type 1 ECG after pilsicainide increased by 9% (an additional 14 cases) and the prevalence of a maxΔJ $\geq$200μV after the test increased by 10% (an additional 16 cases) as compared with using only the standard leads. The majority of cases (23 of 29 in the standard leads and 42 of 45 in the high right precordial leads) with a maxΔJ $\geq$200μV exhibited a typical type 1 ECG. In contrast, cases that showed no obvious morphological ST-T changes (normal ECGs), even when the high right precordial leads were used in the analysis, had an increase in the amplitude of less than 200μV. To the best of our knowledge, there have been few reports describing evidence of positive criteria for the Na^+ challenge test. Our data supports the positive criteria of the pharmacologic test in the consensus report[4] and an increase in the J wave amplitude of greater than 200μV seems to have a meaningful significance for the diagnosis of a drug-induced BS compatible ECG.

Na^+-Channel-Blocker Challenge Test Using Pilsicainide

It has been widely accepted that a shift in the balance of the current, which leads to the loss of the action potential dome in the RV outflow epicardium but not the endocardium, is the mechanism of ST elevation in the right precordial leads in BS.[13] With a reduction in the inward Na^+ currents (I_{Na}), the notch in the epicardial action potentials becomes deeper, producing a voltage gradient between the epicardium and endocardium. This voltage gradient produces ST elevation in the right precordial leads and induces lethal arrhythmias caused by phase 2 reentry.[13] Induction of VF during the drug challenge test or after the administration of Na^+-channel blockers in patients with paroxysmal atrial fibrillation with typical ST-segment elevation has been described.[3,14,15] However, we carefully administered pilsicainide with continuous ECG monitoring and immediately discontinued administration when marked ST-segment elevation, excessive QRS prolongation or ventricular arrhythmias were observed. We completed the drug challenge test safely without any severe adverse events.[4,9]

Recently, an association of BS with atrial fibrillation, atrial vulnerability and supraventricular tachyarrhythmias has been reported.[16–18] Therefore, we performed the drug

challenge test not only in those who exhibited ECG abnormalities, but also in those who had some symptoms and/or various arrhythmias in order to diagnose drug-induced Brugada-type ECGs and/or to evaluate the safety of the drug. We used pilsicainide, which is a pure Na^+-channel blocker and class Ic drug based on the Vaughan Williams classification![9] Other class I anti-arrhythmic agents have ion channel blocking effects not only on the Na^+ channels but also on K^+ channels including the transient outward current (I_{to}), which mediates the spike-and-dome morphology of the epicardial action potential![20,21] By using a pure Na^+ channel blocker, changes in the ST-segment morphology, as viewed on the ECG, may directly reflect the drug's blocking effect on the Na^+ channel.

In regard to the assessment of the J wave amplitude, it is often difficult to determine the J point, especially with the Brugada sign, because of the obscurity of the end of the QRS and the beginning of the T wave. In order to avoid any error in the measurement using manual measurements, we performed a quantitative analysis using a computer algorithm.

Effects of Pilsicainide on ST-Segment Morphology and Elevation

In BS, some investigators have reported that the Brugada sign is more easily detected from the higher right precordium than in the usual standard ECG recording positions![22–25] However, Priori and Napolitano found that this maneuver led to an over-diagnosis of BS![26] Further, the augmentation of ST-segment elevation by Na^+-channel blockers may not be a specific response solely for BS. Peters et al reported that 16% of patients with RV cardiomyopathy respond with ST elevation to the Na^+-channel challenge test[27] and Goda et al reported pilsicainide-induced coronary vasospasms in a patient with a Brugada-type ECG![28] It also appears to be necessary to have a type 1 ECG after pilsicainide administration in order to differentiate a normal variant from BS.

There have been few reports about the prevalence of drug-induced Brugada-type ECGs in a relatively large group of patients with structurally normal hearts or in a healthy population![8,9] Hong et al[10] investigated the response to the ajmaline test in 4 large families with SCN5A mutations. The incidence of a positive test was high in the genetic carriers and low in the genetic non-carriers. Because we did not routinely perform genetic tests, it is unclear whether there was a relationship between the pilsicainide test and the genetic test.

Clinical Implications and Study Limitations

Because the observed drug-induced changes are surrogates for a genetic diagnosis of BS, the true meaning of a positive challenge is unknown and, therefore, of uncertain significance. However, because the present study showed that the ECG response to Na^+-channel blockers exhibited a distinct difference in both the ST-T morphology and response of the J wave amplitude in the majority of cases, we believe that using the pilsicainide challenge test according to our method makes it possible to discriminate between a drug-induced Brugada-type ECG and normal variants.

It is still now an important issue as to whether or not the Na^+ channel challenge test can stratify the risk of cardiac events, so that we can give adequate recommendations or suggestions to our patients. In our study, the patients with an unmasked coved-type ST elevation are all alive. We still need a long-term follow-up of those patients to determine whether or not they will develop cardiac events.

Conclusion

The pilsicainide challenge test performed according to our protocol was safe and helpful for diagnosing drug-induced Brugada-type ECGs. Based on the response recorded in the right precordial leads, including the high right precordial leads, to pilsicainide, a $\max\Delta J \geq 200\mu V$ was associated with a change mainly to a type 1 ECG. In this group there should be great concern for the possible risk of lethal arrhythmias.

References

1. Miyazaki T, Mitamura H, Miyoshi S, Soejima K, Aizawa Y, Ogawa S. Autonomic and antiarrhythmic drug modulation of ST segment elevation in patients with Brugada syndrome. *J Am Coll Cardiol* 1996; **27:** 1061–1070.
2. Brugada J, Brugada P. Further characterization of the syndrome of right bundle branch block, ST segment elevation, and sudden cardiac death. *J Cardiovasc Electrophysiol* 1997; **8:** 325–331.
3. Morita H, Morita ST, Nagase S, Banba K, Nishii N, Tani Y, et al. Ventricular arrhythmia induced by sodium channel blocker in patients with Brugada syndrome. *J Am Coll Cardiol* 2003; **42:** 1624–1631.
4. Wilde AAM, Antzelevitch C, Borggrefe M, Brugada J, Brugada R, Brugada P, et al for the Study Group on the Molecular Basis of Arrhythmias of the European Society of Cardiology. Proposed diagnostic criteria for the Brugada syndrome: Consensus report. *Circulation* 2002; **106:** 2514–2519.
5. Antzelevitch C, Brugada P, Borggrefe M, Brugada J, Brugada R, Corrado D, et al. Brugada syndrome: Report of the second consensus conference: Endorsed by the Heart Rhythm Society and the European Heart Rhythm Association. *Circulation* 2005; **111:** 659–670.
6. Brugada R, Brugada J, Antzelevitch C, Kirsch GE, Potenza D, Towbin JA, et al. Sodium channel blockers identify risk for sudden death in patients with ST-segment elevation and right bundle branch block but structurally normal hearts. *Circulation* 2000; **101:** 510–515.
7. Priori SG, Napolitano C, Gasparini M, Pappone C, Della Bella P, Brignole M, et al. Clinical and genetic heterogeneity of right bundle branch block and ST-segment elevation syndrome: A prospective evaluation of 52 families. *Circulation* 2000; **102:** 2509–2515.
8. Beldner S, Lin D, Marchlinski FE. Flecainide and propafenone induced ST-segment elevation in patients with atrial fibrillation: Clue to specificity of Brugada-type electrocardiographic changes. *Am J Cardiol* 2004; **94:** 1184–1185.
9. Rolf S, Bruns HJ, Wichter T, Kirchhof P, Ribbing M, Wasmer K, et al. The ajmaline challenge in Brugada syndrome: Diagnostic impact, safety, and recommended protocol. *Eur Heart J* 2003; **24:** 1104–1112.
10. Hong K, Brugada J, Oliva A, Berruezo-Sanchez A, Potenza D, Pollevick GD, et al. Value of electrocardiographic parameters and ajmaline test in the diagnosis of Brugada syndrome caused by SCN5A mutations. *Circulation* 2004; **110:** 3023–3027.
11. Task Force of the Working Group on Arrhythmias of the European Society of Cardiology. The Sicilian gambit: A new approach to the classification of antiarrhythmic drugs based on their actions on arrhythmogenic mechanisms. *Circulation* 1991; **84:** 1831–1851.
12. Kodama I, Ogawa S, Inoue H, Kasanuki H, Kato T, Mitamura H, et al. Profiles of aprindine, cibenzoline, pilsicainide and pirmenol in the framework of the Sicilian Gambit. *Jpn Circ J* 1999; **63:** 1–12.
13. Antzelevitch C. The Brugada syndrome: Diagnostic criteria and cellular mechanisms. *Eur Heart J* 2001; **22:** 356–363.
14. Goethals P, Debruyne P, Saffarian M. Drug-induced Brugada syndrome. *Acta Cardiol* 1998; **53:** 157–160.
15. Matana A, Goldner V, Stanic K, Mavric Z, Zaputovic L, Matana Z. Unmasking effect of propafenone on the concealed form of the Brugada phenomenon. *Pacing Clin Electrophysiol* 2000; **23:** 416–418.
16. Eckardt L, Kirchhof P, Loh P, Schulze-Bahr E, Johna R, Wichter T, et al. Brugada syndrome and supraventricular tachyarrhythmias: A novel association? *J Cardiovasc Electrophysiol* 2001; **12:** 680–685.
17. Morita H, Kusano KF, Nagase S, Fujimoto Y, Hisamatsu K, Fujio H, et al. Atrial fibrillation and atrial vulnerability in patients with Brugada syndrome. *J Am Coll Cardiol* 2002; **40:** 1437–1444.

18. Bordachar P, Reuter S, Garrigue S, Caï X, Hocini M, Jaïs P, et al. Incidence, clinical implications and prognosis of atrial arrhythmias in brugada syndrome. *Eur Heart J* 2004; **25:** 879–884.
19. Hattori Y, Hidaka T, Aisaka K, Satoh F, Ishihara T. Effect of SUN 1165, a new potent antiarrhythmic agent, on the kinetics of rate-dependent block of Na channels and ventricular conduction of extrasystoles. *J Cardiovasc Pharmacol* 1988; **11:** 407–412.
20. Antzelevitch C. The Brugada syndrome. *J Cardiovasc Electrophysiol* 1998; **9:** 513–516.
21. Antzelevitch C, Brugada P, Brugada J, Brugada R, Towbin JA, Nademanee K. Brugada syndrome: 1992–2002: A historical perspective. *J Am Coll Cardiol* 2003; **41:** 1665–1671.
22. Sangwatanaroj S, Prechawat S, Sunsaneewitayakul B, Sitthisook S, Tosukhowong P, Tungsanga K. New electrocardiographic leads and the procainamide test for the detection of the Brugada sign in sudden unexplained death syndrome survivors and their relatives. *Eur Heart J* 2001; **22:** 2290–2296.
23. Hisamatsu K, Morita H, Kusano KF, Takenaka S, Nagase S, Nakamura K, et al. Evaluation of the usefulness of recording the ECG in the 3rd intercostal space and prevalence of Brugada-type ECG in accordance with recently established electrocardiographic criteria. *Circ J* 2004; **68:** 135–138.
24. Nakazawa K, Sakurai T, Takagi A, Kishi R, Osada K, Miyazu O, et al. Clinical significance of electrocardiography recordings from a higher intercostal space for detection of the Brugada sign. *Circ J* 2004; **68:** 1018–1022.
25. Meregalli PG, Wilde AAM, Tan HL. Pathophysiological mechanisms of Brugada syndrome: Depolarization disorder, repolarization disorder, or more? *Cardiovasc Res* 2005; **67:** 367–278.
26. Priori SG, Napolitano C. Management of patients with Brugada syndrome should not be based on programmed electrical stimulation. *Circulation* 2005; **112:** 285–291.
27. Peters S, Trummel M, Denecke S, Koehler B. Results of ajmaline testing in patients with arrhythmogenic right ventricular dysplagia-cardiomyopathy. *Int J Cardiol* 2004; **95:** 207–210.
28. Goda A, Yamashita T, Kato T, Koike A, Sagara K, Kirigaya H, et al. Pilsicainide-induced coronary vasospasm in a patient with Brugada-type electrocardiogram: A case report. *Circ J* 2005; **69:** 858–860.

Circ J 2007; **71:** 242–251

Spectral Analysis of Atrial Fibrillation Cycle Lengths
— Comparison Between Fast Fourier Transform Analysis and Autocorrelation Function Analysis Using Multipurpose Physio-Informatic Analysis Software —

Akihiko Shimizu, MD; Takeshi Ueyama, MD; Masahiko Yoshiga, MD; Akira Sawa, MD; Shinichi Suzuki, MD; Naoki Sugi, MD; Masunori Matsuzaki, MD

Background Fast Fourier transform (FFT) analysis is a popular method of spectral analysis of atrial fibrillation cycle lengths (AFCL). Autocorrelation function (ACF) analysis is also available, so the aim of this study was to elucidate the relationship between FFT and ACF analyses in the spectral analysis of AFCLs.

Methods and Results A total of 75 atrial fibrillation (AF) data from 39 patients were subjected to analysis. The dominant frequencies (DFs) from 4 different spectral resolutions of the FFT and peak AFCL from the ACF analysis were compared. In the FFT analysis using rectified signals, the DF was influenced by spectral resolution, no matter how the signals were tapered by the Hanning or Hamming window or filtered with the low-pass filter. There was a significant relationship between the DF from each spectral resolution and the peak AFCL. The DF from the 4,096-point FFT analysis had the strongest relationship to the peak AFCL with the smallest difference, when using 30-s AF data. In a study of the different lengths of the atrial fibrillation data, the DF also had a strong correlation to the peak AFCL with a small difference.

Conclusions The peak AFCL obtained from ACF analysis was not of the same quality as that from FFT analysis, but had the same value as the DF from FFT analysis. (*Circ J* 2007; **71:** 242–251)

Key Words: Atrial fibrillation; Autocorrelation function; Dominant frequencies; Fast Fourier transform analysis; Peak atrial fibrillation cycle length

Atrial fibrillation (AF) is the most frequently occurring arrhythmia requiring treatment. The electrophysiological characteristics of the waveform can be used to classify the arrhythmia, based on the morphology and complexity of atrial activation, and this is the method generally used[1–4] Further, the local fibrillation interval during AF is also very important information for characterization[1–6] These data may be useful for determining the strategy for the AF therapy[6–10] but the measurement of the local fibrillation interval is very labor intensive and there is a risk of data bias when using visual methods. Atrial activation during AF has been frequently described as random or chaotic and recent studies have shown various degrees of organization in AF[11] Thus, spectral analysis of AF intervals has recently become well established and of the several types of spectral analyses used for the characterization of AF, fast Fourier transform (FFT) is the most frequently used[7,10,12–15] However, signal processing and spectral resolution vary among investigators.

We have proposed a new method of spectral analysis, the autocorrelation function (ACF), which is available for analyzing type I AF[16] ACF is a reversed Fourier transformation of the power spectral density, and the power spectral density is a Fourier transformation of the correlation functions, which are determined by the Wiener-Khintchine relation[17] Therefore, the ACF is a so-called reversed Fourier transformation. Mathematically, the values from both methods are the same when the data length is the same. However, the length of the data actually analyzed is limited when AF data are analyzed by spectral analysis. Thus, the relationship between FFT and ACF analyses for the analysis of AF cycle lengths (AFCL) remains unclear.

The aims of this study were to investigate the influence of the different signal processing spectral resolutions, and length of the AF data on the spectral analysis, and then to elucidate the relationship between the FFT and ACF analyses, using multipurpose physio-informatic analysis software (BIMUTAS II for Windows, Kissei Comtec, Ltd, Tokyo, Japan).

(Received March 2, 2006; revised manuscript received October 30, 2006; accepted November 13, 2006)

Division of Cardiology and Faculty of Health Sciences, Yamaguchi University Graduated School of Medicine, Yamaguchi, Japan
Mailing address: Akihiko Shimizu, MD, Faculty of Health Sciences, Yamaguchi University Graduated School of Medicine, 1-1-1 Minami-Kogushi, Ube 755-8505, Japan. E-mail: ashimizu@yamaguchi-u.ac.jp

Methods

Patients

The study protocol was approved by the regional ethics committee and written consent was given by all 39 patients enrolled in the study (28 males, 8 females, 59±7 years old). The subjects were placed in 2 groups: the induced group (21 patients) and persistent group (18 patients). None of the patients had any organic heart disease, but all had a history of atrial flutter (AFl) or AF. All patients underwent an electrophysiological study prior to catheter ablation of the AFl or intracardiac cardioversion.

The electrophysiological study was performed in the fasting state, and all previous antiarrhythmic agents were

discontinued for at least 5 half-lives. An intravenous propofol infusion was used to achieve general anesthesia.

Recordings

A standard 6F decapolar catheter with 10 2-mm width electrodes and a 2-mm interelectrode spacing was introduced via the right femoral vein or left or right subclavian vein. The catheters were positioned in the high lateral right atrium (HRA), low lateral right atrium (LRA), His bundle region and coronary sinus. The 12-lead surface ECG was recorded simultaneously with the intracardiac electrograms. The bipolar endocardial electrograms were recorded from each of the 5 closely spaced bipolar pairs of electrodes filtered through a 30–400 Hz filter, with a sampling interval of 1 kHz, using a computed electric recorder (EPL00372-001-07, EP LAB, Quinton, Canada).

When spontaneous or induced AF lasted for more than 10 min, the atrial electrograms during AF were continuously recorded for 30–180 s.

Analysis

We used the methods previously reported for analyzing the data![6] First, we selected the AF episode on the screen of EP LAB from the right atrium. Second, we transferred the selected data to a hard disk using a program available in EP LAB. Third, binary data from the atrial electrograms were retrieved from the hard disk of the EP LAB system using an optical disk, and then transformed into compatible data for BIMUTAS II on a personal computer (Value Star NX, NEC, Tokyo, Japan). Four, we arbitrarily selected 30-s data from the atrial electrograms from the HRA and LRA, then analyzed those data.

Signal Processing

The raw data were subjected to rectification, then to low-pass filtering (cutoff 20 Hz) by an installed program in BIMATUS II, in order to remove the high-frequency potentials.

Spectral Analysis

Each set of AF data was analyzed by both FFT and ACF using installed software in BIMUTAS II. A 5-s data set was selected arbitrarily and only used for a representative episode to compare relatively organized and disorganized atrial electrograms. A 30-s set of data was used to study the relationship between the dominant frequencies (DF) and peak AFCL.

FFT Analysis

The FFT analysis was performed using the raw, rectified and then low-pass filtered signals. It was also performed with a Hamming or Hanning window. Finally, FFT analysis was performed for 5- or 30-s sets of data using different spectral analyses with an ensemble mean value; 1,024-point FFT (spectral resolution: 0.98 Hz), 2,048-point FFT (spectral resolution: 0.49 Hz), 4,096-point FFT (spectral resolution: 0.24 Hz) and 8,192-points FFT (spectral resolution: 0.12 Hz). The amplitude was expressed as the power spectral density (V^2). The relative amplitudes of the peaks from each FFT were compared, and the frequency of the peak with the largest amplitude was assigned to be the DF, as previously reported![10,13]

With BIMUTAS II, when the FFT point (spectral resolution) exceeded the duration of the AF data selected, 0-padding was performed for the residual points. If the sampling rate was 1,000 Hz, 0-padding was performed for 3,192 (=8,192–5,000) points when a 5-s data set was analyzed using 8,192-point FFT. The signal-averaging process was performed when the length of the data analyzed exceeded the FFT point. For example, when a 30-s data set was analyzed using a 4,096-point FFT, the signal-averaging was performed with 7 segments and the 0-padding was performed for 1,328 points (=30,000–4,096×7).

ACF Analysis

The ACF analysis was also performed using the same raw, rectified and then low pass filtered signals as in the FFT analysis.

The ACF was defined as: $Rxx(\tau)=\int_{-\infty}^{\infty} Pxx(f)e^{i2\pi f\tau}d\tau$

Where Rxx (t) is the ACF, Pxx (f) is the power spectrum, t is time displacement, f is cyclical frequency and i is the index. With BIMUTAS II, the ACF analysis was performed by the indirect method of computing autocorrelation estimates based on the Weiner-Khinchine relation![7] Thus, the ACF was computed by taking the inverse Fourier transformation of the autospectrum estimate. When t was 0, Rxx (0) was regulated as 1. Further, the number 2^n, which was greater than the number of points that were analyzed, was selected as the FFT point for the ACF, and 0-padding was performed for the residual points. For example, when ACF was performed for a 5-s set of data at a sampling rate of 1,000 Hz, 8,192-points were selected as the FFT point and then 0-padding was performed for the residual 3,192 points (=8,192–5,000 points). Similarly, when ACF was performed for a 30-s set of data at a sampling rate of 1,000 Hz, 32,768-points were selected as the FFT point, and then 0-padding was performed for 2,768 points (=32,768–30,000).

The values of the first peak of the coefficient Rxx (R), on the positive side of the autocorrelogram was taken as the peak AFCL, as previously reported![6]

AF was defined as a rapid atrial rhythm characterized by a variability in the beat-to-beat cycle length, polarity, configuration and amplitude of the recorded bipolar atrial electrograms! Persistent AF was defined as AF that lasted more than 1 month and less than 1 year.

To ensure the reliability of DF detection and peak AFCL, 3 data sets (2 for the induced group and 1 for the persistent group) with a coefficient R <0.1 for ACF were discarded from the subsequent analysis because of their ambiguity, in order to avoid any artifact and/or poor recorded signals. Thus, 40 episodes from the induced group and 35 from the persistent group were subsequently analyzed.

We determined the DF obtained from the different spectral resolutions of the FFT analysis and the peak AFCL from the ACF. We studied the relationship between the DF from the FFT and peak AFCL from the ACF, using the same rectified, then low-pass filtered atrial electrograms during 30 s of AF. Further, the length of the AF data analyzed should have influenced the FFT point (spectral resolution) in both the FFT and the ACF analyses. Thus, we also compared the DF from the FFT and peak AFCL from the ACF, using the same rectified then low-pass filtered atrial electrograms during 5, 10, 30, and 32.8 s of 10 episodes of AF selected arbitrarily. Because the number of 2^n, which was greater than the number of points that were analyzed, was selected as the FFT point for the ACF in BIMUATAS II, 8,192 points were selected as the FFT point for the 5-s data, 16,384 points for the 10-s data, 32,768 points for the 30-s (30 s-I), and 32,768 points for the 32.8-s